JOURNAL OF GEOPHYSICAL RESEARCH, VOL. 105, NO. E3, PAGES 7053–7070, MARCH 25, 2000

Diaspores and related hydroxides: Spectral-compositional properties and implications for Mars

Edward A. Cloutis

Department of Geography, University of Winnipeg, Winnipeg, Manitoba, Canada

James F. Bell III

Department of Astronomy, Cornell University, Ithaca, New York

Abstract. Differences in spectral reflectance properties (0.3-26 μm) of a suite of metal hydroxides (gibbsite, böhmite, diaspore, goethite, and manganite) have been found to be a function of both structural and compositional differences between these minerals. The properties of the O-H stretching fundamental bands in particular can be used to identify the presence of these minerals and to discriminate isostructural and heteromorphous species. This is due to the fact that the O-H stretching fundamental bands are very intense in these minerals and occur at longer wavelengths than those of other minerals, and also due to the fact that these metal hydroxides lack strong absorption bands at shorter wavelengths. In the case of dimorphous minerals such as böhmite (γ-AlO(OH)) and diaspore (α-AlO(OH)), differences in the wavelength positions of O-H stretching fundamental bands can be of the order of 0.1-0.3 μm. Reflectance spectra of metal hydroxide-bearing "ores" (bauxites) and impure samples indicate that accessory phases, in particular iron-bearing minerals, have a more pronounced effect on spectral reflectance toward shorter wavelengths. Intimate mixtures of diaspore + orthopyroxene indicate that diaspore abundances as low as 5 wt % (or less) can be detected by the appearance of characteristic absorption bands at 3.33 and 3.41 μm. This finding has particular relevance to the study of near-infrared spectra of Mars, in that the conditions which favor diaspore formation on the Earth may have also been prevalent early in Mars' history. If diaspore did form on Mars in the past, it is likely to have persisted to the present.

1. Introduction

Metal hydroxides are common constituents on the Earth's surface [e.g., *Deer et al.*, 1962]. They are of economic importance as major sources of metal (e.g., Al), as well as being useful indicators of metamorphic/hydrothermal conditions [*Bárdossy*, 1982; *Patterson et al.*, 1986]. The reasons for undertaking a study of the spectral properties of aluminum- and other common metal-bearing hydroxides includes their economic importance and hence the possibility of detecting and discriminating terrestrial deposits using optical or infrared remote sensing [e.g., *Crowley*, 1984].

In addition, the relationship of these minerals to aqueous weathering environments on the Earth [e.g., *Valeton*, 1972; *Bárdossy*, 1982; *Bárdossy and Aleva*, 1990; *Cornell and Schwertmann*, 1997], coupled with the widespread but indirect (geomorphological) evidence for wetter conditions prevailing on Mars in its past [e.g., *Pollack et al.*, 1987; *Squyres and Kasting*, 1994; *Carr*, 1996], suggest that these minerals may have formed on the surface of Mars in the past and may provide unique indicators of previous climatic conditions on that planet. Simple metal hydroxides, particularly aluminum hydroxides, are common end products of persistent and intense weathering in the presence of water [*Valeton*, 1972; *Bárdossy*, 1982]. If such minerals could be identified on Mars, they would yield insights into paleoenvironmental conditions on the planet. Such reconstructions would depend on our ability to discriminate different metal hydroxides from one another and from other minerals, as well as to identify their presence when associated with other phases, some of which may be poorly crystalline and/or spectrally dominant.

Reflectance spectroscopy has proven to be one of the most useful techniques for deriving mineralogical information for remote surfaces such as Mars [e.g., *Roush et al.*, 1993; *Bell et al.*, 1997; *Calvin*, 1997]. Reflectance spectroscopy can provide direct mineralogical information, in contrast to other techniques such as alpha proton X ray spectrometry (APXS) which provide elemental abundances from which plausible mineralogies must be inferred [*Rieder et al.*, 1997]. Compared to thermal infrared emittance spectroscopy [e.g., *Farmer*, 1974], which is sensitive primarily to coarsely crystalline and/or primary (unaltered) silicate phases, reflectance spectroscopy provides diagnostic information on secondary weathering products and/or poorly crystalline phases. These secondary products are often dominated spectrally by ferric iron (Fe^{3+}), which is an important and abundant component of the Martian surface [e.g., *Banin et al.*, 1992; *McSween et al.*, 1999]. Interpretation of recent telescopic spectra of Mars at these wavelengths are consistent with the presence of diaspore on Mars (J.F. Bell et al., Identification of hydroxyl bearing minerals on Mars, submitted to *Science*, 1999) (hereinafter referred to as (Bell et al., submitted manuscript, 1999)), and may provide perhaps the first definitive identification of the long-known "hydrated mineral component" on that planet's surface [*Pimentel et al.*, 1974; *Anderson and Tice*, 1979].

Paper number 1999JE001188.
0148-0227/00/1999JE001188$09.00

In addition, reflectance spectroscopy can provide information on the presence and crystallographic/structural configuration of low atomic weight elements such as hydrogen, and molecules such as OH and H_2O in minerals; such determinations are beyond the capabilities of most other analytical techniques such as APXS [*Rieder et al.*, 1997]. Many O-H and H-O-H fundamental, combination, and overtone absorption bands fall below the wavelength limits of typical thermal infrared spectral systems. Thus we view reflectance spectroscopic techniques as being complementary to other techniques, and in some instances as being able to provide unique information.

The original impetus for this study was to attempt to identify the cause of specific absorption features seen in Earth-based telescopic spectra of Mars in the 3- to 4-μm region which have been tentatively attributed to diaspore (α-AlO(OH)) (Bell et al., submitted manuscript, 1999) and to attempt to confirm the possible previous detections of other metal hydroxides, primarily goethite, on the surface of Mars [*Bishop et al.*, 1993; *Geissler et al.*, 1993; *Murchie et al.*, 1993; *Kirkland and Herr*, 1998]. Identification of specific metal hydroxides would bolster the geomorphological evidence for wetter conditions early in Mars' history, help to explain the ultimate fate of this water [*Clifford*, 1993; *Carr*, 1996], and assist in constraining models of the planet's climatic evolution, given the formation conditions associated with specific metal hydroxides [*Stumpf et al.*, 1950; *Deer et al.*, 1962; *Wefers*, 1967a, b, c; *Bárdossy*, 1982].

In order to address these issues, a number of naturally occurring metal hydroxide minerals were characterized using a range of analytical techniques. The goal was to determine the unique spectral-compositional properties of the samples. This study focused on diaspore because of its tentative identification in Mars telescopic spectra as well as its general plausibility as a surface mineral phase in the Martian environment. The samples that were studied included both pure diaspores and diaspore-rich ores as well as bauxite ores; the latter two being useful for understanding the spectrum-altering effects of minerals commonly associated with aluminum hydroxides in terrestrial deposits. The other minerals were included in order to determine whether diaspores do exhibit unique spectral properties relative to closely related minerals. In addition, the reflectance spectra of a series of diaspore+palagonite and diaspore+orthopyroxene mixtures were analyzed in order to constrain detection limits for diaspore in the presence of basaltic minerals and weathering products thought to be present on the Martian surface based on previous studies [*Singer*, 1982; *Morris et al.*, 1993; *Bell et al.*, 1993].

2. Experimental Procedure

A total of 13 metal hydroxide samples were included in this study and are numbered with an "OOH" prefix and three number suffix. They include aluminum hydroxides, bauxite ores, and other metal hydroxides. The bauxite ores are OOH001 (from Guyana) and OOH002 (from Arkansas); both are gibbsite-rich. The aluminum hydroxide minerals include gibbsite from Brazil (α-$Al(OH)_3$; OOH004), and böhmite from France (γ-AlO(OH); OOH005). Three essentially pure diaspores (α-AlO(OH)) were acquired from the Smithsonian Institution National Museum of Natural History: OOH011 (from South Africa; manganoan; NMNH #140594), OOH012 (from Massachusetts; NMNH #81900-1), and OOH013 (from California; NMNH #140597). Diaspore-rich samples were obtained from a commercial supplier (OOH007, from Nevada), and from Alcan International Limited: OOH008 and OOH009 (both from China), and OOH010 (from Greece). The other metal-bearing hydroxides which were included are goethite from Michigan (α-FeOOH; OOH003), and manganite from Canada (MnOOH; OOH006).

Sample preparation in all cases involved hand picking of a purified fraction (where possible), crushing of the samples in an alumina mortar and pestle, and dry sieving to obtain <45 and 45-90 μm size fractions. In four cases, OOH008, 009, 012, and 013, <5 μm fractions were obtained by wet sieving the <45 μm fraction with acetone (after the <45 μm size fraction had been spectrally characterized).

In order to determine the relationship between the spectral and compositional properties of the samples, and to understand the possible spectral interferences due to accessory phases, <45 μm sized splits of the samples were characterized by X ray diffraction, differential scanning calorimetry, thermogravimetry, and infrared transmission spectroscopy by Alcan International Limited. These data served to ascertain the abundance and nature of the hydroxide phase(s) present in the samples as well as for determination of OH content. The X ray diffraction data were acquired with a Scintag XDS-2000; operating conditions were a Cu Kα radiation source at 45 kV and 40 mA, with the sample placed in vertical sample holder. Differential scanning calorimetry and thermogravimetry were performed using a DuPont Model 2100 Thermal Analyzer. For differential scanning calorimetry the samples were placed in aluminum pans with perforated lids and heated at 20°C/min. For thermogravimetry the samples were placed in platinum pans and heated at 20°C/min with an airflow of 40 mL/min. The infrared transmission spectra were measured using a Bomem MB-100 instrument. The mineral samples were ground with KBr (~1% sample/KBr) and formed into 13 mm diameter pellets under a pressure of 10 tons. Additional information on the analytical instrumentation is given by *Authier-Martin et al.* [1999].

Elemental abundances were determined using inductively coupled plasma atomic emission spectroscopy (ICP-AES) by Alcan International Limited (Table 1). The samples were fused in molten KOH and diluted in acid for ICP-AES analysis after loss on ignition determinations. Mineral abundances in the samples (Table 2) were determined from a combination of ICP-AES, X-ray diffraction (XRD), thermogravimetric analysis (TGA), and differential scanning calorimetry (DSC) data, whereby elemental abundances and known phases were combined in an integrated analysis to constrain mineral abundances [*Authier-Martin et al.*, 1999]. Samples OOH001 and OOH002 were found to be composed predominantly of gibbsite; the presence of other phases is apparent from the relatively high abundances of additional elements such as Si, Ti, and Fe, the low elemental totals, the differences in volatile loss on ignition between the actual and calculated values, and XRD results. OOH003 is nearly pure goethite although the presence of a minor amount of hematite (<1%) and silicates is indicated. OOH004 is predominantly gibbsite although the overall elemental abundance is lower than expected. OOH005 is mainly böhmite with significant amounts of clay minerals (mostly kaolinite) and hematite. The intimate association of these phases in the sample precluded preparation of a higher purity separate. OOH006 is nearly pure manganite; no other phases are indicated by XRD. The volatile loss on ignition run did not allow for complete characterization of the total volatile content, however. On the assumption of pure manganite, the elemental total is close to 100%. OOH007 is a diaspore-rich sample containing abundant pyrophyllite which accounts for the high Si content and low overall elemental total. OOH008, 009, and 010 are all diaspore-rich "ores" composed predominantly of diaspore (Table 2). Samples OOH011, 012, and 013 were found to be essentially pure (>99%) diaspore.

Table 1. Compositions of the Samples Used in This Study

	Sample ID, Major Phase												
	OOH001 Gibbsite	OOH002 Gibbsite	OOH003 Goethite	OOH004 Gibbsite	OOH005 Böhmite	OOH006 Manganite	OOH007 Diaspore	OOH008 Diaspore	OOH009 Diaspore	OOH010 Diaspore	OOH011 Diaspore	OOH012 Diaspore	OOH013 Diaspore
Al_2O_3	58.56	50.81	1.22	57.04	47.79	0.75	46.84	70.27	73.86	56.10	83.68	81.22	83.87
Fe_2O_3	0 54	7.55	89.29	0.08	16.00	0.03	0.13	0.27	1.15	18.71	0.12	0.62	0.49
SiO_2	1 83	4.25	1.40	0.47	19.38	0.31	37.29	7.02	2.69	3.47	0 19	0.28	0.08
TiO_2	1 99	2.08	0.07	0 03	2.08	0.32	0.94	5.47	3.74	2.65	0 01	0.15	0.08
CuO	0.01	0.01	0.01	0.02	0.02	0.06	0.03	0.02	0.02	0.01	0.05	0.06	0.07
MgO	0 02	0.06	0.19	0.02	0.02	0.06	0.03	0.07	0 05	0.13	0.02	0.04	0.06
CaO	0.05	0.15	0.06	0.05	0.21	0.24	0.09	0.08	0.08	1.81	0.04	0.90	0.06
MnO	0.003	0.12	0.21	0.02	0.10	79.13	0.02	0.01	0 001	0.08	0.15	0.01	0.02
NiO_2	0.002	0.003	0.01	0.005	0.02	0.09	0.01	0.01	0.01	0.08	0.02	0.01	0.01
V_2O_5	0.02	0.05	0.004	0.001	0.05	0.00	0.04	0.05	0.06	0.10	0.001	0.02	0.02
ZnO	0 01	0.01	0.03	0.01	0 03	0.05	0.02	0.03	0.02	0.01	0.02	0.01	0.02
ZrO_2	0.16	0.22	0.002	0.002	0.08	0.01	0.02	0.26	0.25	0.07	0.002	0.003	0.001
Na_2O	0 34	0.25	0.48	0.00	0.80	0.82	0.59	1.21	0.54	0.82	0.47	1.10	0.46
L.O.I.[a]	32.7	30.7	9.8	35.3	13.7	≥11.3	8.6	14.5	14.5	13.4	15.1	14.9	14.9
L.O.I.[b]	31.0	26 9	10.0	30.2	10.2	18.9	8.3	12.4	13.0	9.9/12.0	14.8	14.3	14.8
L O.I.[b]	Gi	Gi	Go	Gi	Bo+Go	Ma	Di	Di	Di	Di/Di+Bo	Di	Di	Di
Total[a]	96.235	96.263	102.776	93.048	100.280	93.170	94.65	99.27	96.97	97.44	99.873	99.323	100.141
Total[b]	94.535	92.463	102.976	87.948	96.78	100.770	94.35	97.17	95.471	93.94/ 96.04	99.573	98.723	100.041

All Fe reported as Fe_2O_3. National Museum of Natural History sample identification code 140594 for OOH011, 81900-1 for OOH012, and 140597 for OOH013. Alcan # 4080 for OOH008, 4086 for OOH009, and 30941-K for OOH010.

[a] L.O.I., measured loss on ignition: 25-1000°C (wt %).

[b] L.O.I., calculated loss on ignition based on the following scenarios. Gi, all Al_2O_3 as gibbsite; Go, all Fe_2O_3 as goethite; Bo, all Al_2O_3 as böhmite; Di, all Al_2O_3 as diaspore; Ma, all MnO as manganite; Di+Go, all Al_2O_3 as diaspore and all Fe_2O_3 as goethite; Bo+Go, all Al_2O_3 as böhmite and all Fe_2O_3 as goethite.

Reflectance spectra of the samples (<45 and 45-90 μm size fractions) were measured at the NASA-supported Reflectance Experiment Laboratory (RELAB) spectrometer facility at Brown University [*Reflectance Experiment Laboratory (RELAB)*, 1996]. The spectra were measured by two instruments: the shorter wavelength spectra (0.3-2.5 μm) were measured using the UV-vis-near-infrared bi-directional spectrometer [*Pieters*, 1983] relative to halon at i=30°, e=0°, and 5 nm resolution. The 2.5-25 μm spectra were measured using the Nicolet 740 Fourier transform infrared spectrometer relative to brushed gold at i=30°, e=30° and spectral resolution decreasing from 0.6 nm at 2.5 μm to 129 nm at 25 μm. The spectra were merged at 2.5 μm. See *Pieters* [1983] and *Reflectance Experiment Laboratory (RELAB)* [1996] for details on the instrumentation and data acquisition procedures. The RELAB spectra were measured in air while the Nicolet spectra were measured in a dry nitrogen atmosphere.

Wavelength positions of absorption band minima in the RELAB spectra were determined by fitting a third-order polynomial to between 10 and 20 data points on either side of a visually determined (approximate) band minimum. Varying the number of data points used in the fitting caused band positions to vary by generally less than 5 nm. In some cases, the absorption bands were not clearly resolvable due to overlaps from adjacent absorption bands or excessive noise in the data. In these cases, band positions are approximate and are indicated as such in the ensuing discussion. Wavelength positions of absorption bands in the spectra of other investigators were either measured off the published spectra or provided in the accompanying articles. In these cases absorption band positions may be less accurate than for the RELAB spectra. No continuum removal was applied because of the diversity of spectral shapes and uncertainties in how best to construct a physically meaningful continuum.

Table 2. Approximate Abundances of Phases Present in Diaspore-Rich "Ores" OOH008-010

Phase Abundance, wt %	OOH008	OOH009	OOH010
Diaspore	82-88	82-88	
Diaspore + böhmite			71-76
Quartz	4	4	2
Kaolinite	4	4	4
Anatase	4	4	3
Hematite	<1	<1	12-15
Calcite			2
Others	<1	<1	<1

3. Spectral-Compositional Relationships

3.1. Gibbsite (α-$Al(OH)_3$)

Gibbsite is the predominant phase in samples OOH001, 002, and 004 (Table 1). It consists of edge sharing hydroxyl octahedra with two thirds of the octahedral sites occupied by aluminum atoms [*Deer et al.*, 1962; *Kostov*, 1968]. The reflectance spectra exhibit the most prominent absorption bands in the 1.4-1.6, 2.2-2.4, and 2.7-3.0 μm regions (Figure 1). These spectra are similar to gibbsite reflectance spectra measured by other investigators [*Hunt et al.*, 1971; *Crowley*, 1984; *Grove et al.*, 1992].

The bands in the 2.7-3.0 μm region are attributable to the gibbsite as well as the accessory phases that are present. The five strongest bands (near 2.76, 2.83, 2.88, 2.94, and 2.96 μm) are similar to those seen in transmission spectra of natural and synthetic gibbsite measured by other investigators and are all apparently attributable to O-H stretching fundamentals (Table 3). The multiplicity of bands is due to the fact that a number of distinct O-H bonding distances exist in

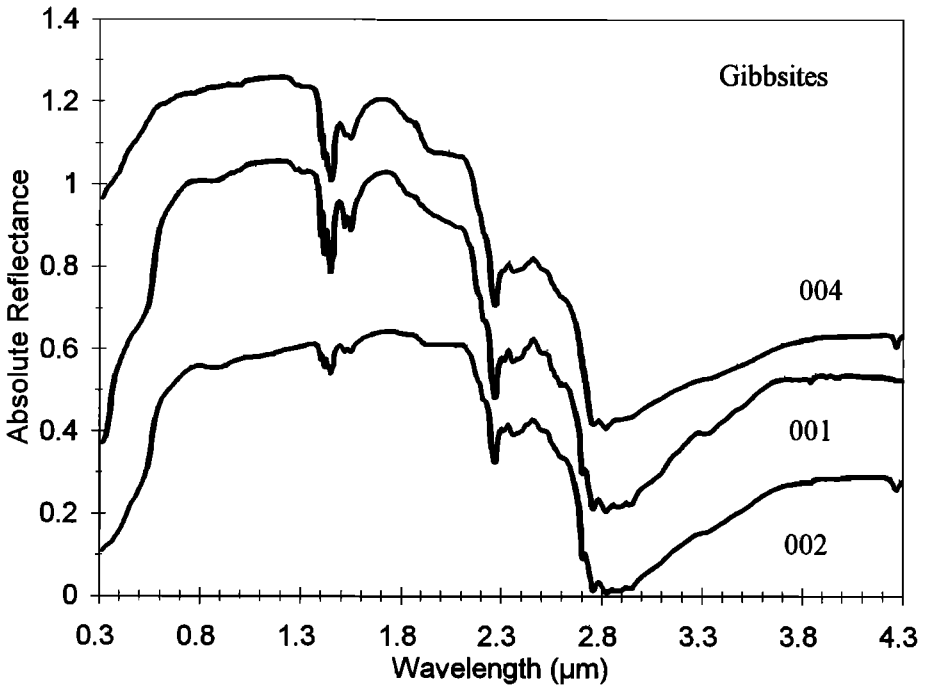

Figure 1. Plot of 0.3-4.3 μm reflectance spectra of <45 μm size fractions of gibbsite-rich samples OOH001, 002, and 004. The spectra have been vertically offset for clarity as follows: OOH001, +0.2; OOH004, +0.4.

gibbsite [*Rouquerol et al.*, 1970; *Ryskin*, 1974]. The number and relative intensity of the bands varies from sample to sample; these variations are probably due to a combination of structural differences between samples and differences in spectral resolution and quality of the published spectra. The transmission spectra are generally similar to the reflectance spectra, although slight differences in positions of the absorption bands are present (Table 3). In almost all cases, the transmission and reflectance spectra of the same sample exhibit the same number of resolvable absorption features.

At shorter wavelengths the gibbsite spectra exhibit at least two bands near 2.27 and 2.36 μm. These bands are probably due to a combination of the Al-O-H stretching and O-H stretching fundamentals (Table 3) [*Hunt and Salisbury*, 1970; *Hunt et al.*, 1971; *Hunt*, 1979]. The absence of a prominent 1.9 μm band is attributable to the absence of H_2O molecules in the structure [*Hunt*, 1979]. The gibbsite spectra also exhibit two sets of bands in the 1.4-1.6 μm region. The two relatively weak bands at 1.52 and 1.55 μm are attributed to a combination of the second overtone of the O-H bending vibrations and the O-H stretching fundamentals. There are at least five resolvable bands located at 1.40, 1.42, 1.44, 1.45, and 1.46 μm which can be attributed to overtones or combinations of the O-H stretching fundamentals (Table 3).

At wavelengths shortward of 1.3 μm, pure gibbsite is relatively featureless. The lower overall reflectance below 2 μm and the reflectance decrease below ~0.6 μm are most prominent in the sample with the highest iron content (OOH002). These spectral characteristics are ascribed to iron oxide/hydroxide phases which impart an overall red color to the sample and are intimately associated with the gibbsite. These effects are also seen, to a lesser extent, in the OOH001 spectrum.

3.2. Böhmite (γ-AlO(OH))

Böhmite is compositionally identical to diaspore. Structurally, it consists of double sheets of oxygen octahedra with aluminum at their centers. The sheets are composed of chains of octahedra which share edges or corners, depending on direction. Corner-shared oxygen atoms are hydrogen bonded to two similar oxygens in a neighboring sheet. This differs from diaspore where every oxygen atom is hydrogen bonded, and in the nature of the packing of the oxygen atoms [*Deer et al.*, 1962].

The spectral properties of böhmite have been studied by a number of investigators in the mid- and far-infrared (see references in Table 4). Böhmite invariably exhibits two absorption bands near 3.03 and 3.23 μm due to O-H stretching fundamentals (Table 4). While the data suggest that there is little variation in band positions, some investigators suggest that these bands may shift to longer wavelengths with increasing degree of crystallinity [*Jónás et al.*, 1973]. As in the case of diaspore, the bridging hydrogen atoms between the layers are not symmetrically positioned between the bridged oxygens. This leads to two O-H stretching fundamentals with different energies [*Kolesova and Ryskin*, 1962; *Rouquerol et al.*, 1970; *Ryskin*, 1974]. The intensity and distinctive nature of these bands is apparent in Figure 2 for sample OOH005. The bands in the 2.7-2.8 μm region are attributable to the other phases present in this sample, as evidenced by the presence of additional elements such as Si and Fe and a higher than expected loss on ignition (Table 1).

By analogy with other aluminum hydroxides, we expect additional absorption bands in the 1.4 μm region due to Al-O-H and O-H combination bands in the 2.3 μm region, and a relatively featureless spectrum shortward of 1.3 μm. However, due to the significant

Table 3. Wavelength Positions of O-H Stretching and Bending Fundamental Absorption Bands and Various Combinations and Overtones for Gibbsite

Band Positions, μm	Sample Type	Spectral Type[a]	References
	Al-O-H Stretching Fundamentals		
12.3, 12.7			1-7
	O-H Bending Fundamentals		
9.8, 10.4, 11.0			1-7
	O-H Stretching Fundamentals		
2.765, 2.842, 2.917, 2.960, 2.975	synthetic gibbsite	T	1
2.765, 2.842, 2.917, 2.960, 2.975	gibbsitic bauxite	T	1
2.76, 2.83, 2.89, 2.95	gibbsitic bauxite	T	2
2.765, 2.842, 2.917, 2.975	synthetic gibbsite	T	3
2.768, 2.841, 2.903, 2.950, 2.966	natural gibbsite	T	4
2.765, 2.843, 2.917, 2.960	synthetic gibbsite	T	5
2.762, 2.833, 2.897, ~2.95	natural gibbsite	T	6
2.762, 2 835, 2.893, 2.945, 2.960	OOH001	T	7
2.760, 2.824, 2.882, 2.94	OOH001, <45 μm	R	7
2.760, 2.820, 2.840, 2.940	OOH001, 45-90 μm	R	7
2 762, 2.835, 2.896, 2.946, 2.961	OOH002	T	7
2.760, 2.830, 2.880, 2.942	OOH002, <45 μm	R	7
2.760, 2.822, 2.878, 2.940	OOH002, 45-90 μm	R	7
2.762, 2.836, 2.886	OOH004	T	7
2.76, 2.822, ~2.88, ~2.94	OOH004, <45 μm	R	7
2.757, 2.820, 2.943	OOH004, 45-90 μm	R	7

Combination/Overtone Band Position, μm	Assignment
2.36	Al-O-H stretching + O-H stretching fundamental
2.27	Al-O-H stretching + O-H stretching fundamental
1.55	Second overtone of O-H bending + O-H stretching fundamental
1.52	Second overtone of O-H bending + O-H stretching fundamental
1.46	Overtone/combination of O-H stretching fundamental
1.45	Overtone/combination of O-H stretching fundamental
1.44	Overtone/combination of O-H stretching fundamental
1.42	Overtone/combination of O-H stretching fundamental
1.40	Overtone/combination of O-H stretching fundamental

References are 1, *Frederickson* [1954]; 2, *Jónás and Solymár* [1970]; 3, *Hartert and Glemser* [1956]; 4, *Moenke* [1962]; 5, *Rouquerol et al.* [1970]; 6, *Rudnitskaya and Ziborova* [1967]; 7, this study.

[a] R, reflectance spectral data; T, transmission spectral data.

amount of accessory phases in the sample, these features cannot be uniquely attributed to böhmite. The best evidence for lower wavelength combination and overtone bands are the series of weak bands in the 2.3 μm region; some of these may be attributable to combinations of the O-H bending and stretching fundamentals. The influence of hematite on the spectrum at shorter wavelengths is also apparent [*Sherman et al.*, 1982; *Morris et al.*, 1985].

The spectral properties of böhmite have also been studied as a function of temperature. It has been found that as temperature increases, the intensities of the O-H stretching bands near 3.03 and 3.23 μm decrease, the bands become wider, and move to shorter wavelengths [*Fripiat et al.*, 1967a, b; *Ryskin*, 1974].

3.3. Diaspore (α-AlO(OH))

The focus of this study is the diaspores, and hence their spectra will be discussed in greater detail. The structure of diaspore consists of distorted oxygen octahedra (with aluminum at their centers) which are joined at the edges to form a double chain. Unlike gibbsite, all of the octahedra are occupied by aluminum atoms. These chains are interconnected by shared octahedron corners to form a three-dimensional framework. Hydrogen atoms connect oxygen atoms on adjacent chains. The hydrogen atoms do not lie in a direct line between these oxygen atoms and are more closely bonded to one of the two oxygen atoms. The hydrogen-oxygen distances are also shorter than those in the other aluminum hydroxides [*Kolesova and Ryskin*, 1962; *Ryskin*, 1974]. Unlike böhmite, every oxygen atom is hydrogen bonded to one other oxygen (in böhmite half of the oxygens are not involved in hydrogen bonding while the other half are hydrogen bonded to two other oxygen atoms) [*Deer et al.*, 1962; *Kolesova and Ryskin*, 1962].

The 0.3-4.3 μm reflectance spectra of pure diaspores and diaspore-rich samples are shown in Figures 3 and 4, respectively. The pure diaspore spectra are very similar beyond 1.3 μm and match closely the diaspore spectrum of *Crowley* [1984] and to a lesser extent those of *Hunt et al.* [1971]. The spectra exhibit very high overall reflectance between ~0.4 and 1.4 μm. Reflectance decreases beyond 1.4 μm toward the O-H fundamental stretching bands near 3 33 and 3.41 μm. The positions of these absorption band minima in the transmission and reflectance spectra are listed in Tables 5 and 6, respectively. The manganoan diaspore (OOH011) exhibits an additional absorption feature near 0.5 μm which is probably attributable to Mn^{3+} electronic transitions [*Vempati et al.*, 1995].

The presence of OH dominates the spectral properties of diaspore below ~5 μm. Table 7 lists the positions of the major fundamental and combination/overtone absorption bands seen in diaspore spectra and their assignments [*Hartert and Glemser*, 1956; *Kolesova and Ryskin*, 1962; *Caillère and Pobeguin*, 1966; *Tsuchida and Kodaira*, 1990].

The spectra exhibit a well-defined absorption feature near 1.8 μm, close to the 1.9 μm water band of hydrated minerals. It appears to

Table 4. Wavelength Positions of O-H Stretching Fundamental Absorption Bands and Various Combinations and Overtones for Böhmite

Band Positions, μm	Sample Type	Spectral Type[a]	References
	O-H Bending Fundamentals		
8.7, 9.3			1-10
	O-H Stretching Fundamentals		
3.065, 3.247	böhmite, synthetic	T	1
3.04, 3.23	böhmite-rich bauxites	T	2
3.033, 3.236	böhmite	T	3
3.058, 3.241	böhmite, synthetic, aged	T	4
3.044, 3.226	böhmite, natural	T	5
3.067, 3.247	böhmite, synthetic	T	6
3.040, 3.236	böhmite, natural	T	7
3.067, 3.257	böhmite, synthetic	T	8
3.040, 3.257	böhmite, synthetic	T	8
3.066, 3.248	böhmite, natural	T	8
3.041, 3.231	OOH005	T	9
3.028, 3.210	OOH005, <45 μm	R	9
3.023, 3.208	OOH005, 45-90 μm	R	9
~3.06, ~3.25	six böhmitic bauxites	T	10

References are 1, *Frederickson* [1954]; 2, *Jónás and Solymár* [1970]; 3, *Fripiat et al.* [1967a]; 4, *Kolesova and Ryskin* [1962]; 5, *Moenke* [1962]; 6, *Rouquerol et al.* [1970]; 7, *Rudnitskaya and Ziborova* [1967]; 8, *Sato* [1962]; 9, this study; 10, *Jónás et al.* [1973].

[a] R = reflectance spectral data; T = transmission spectral data.

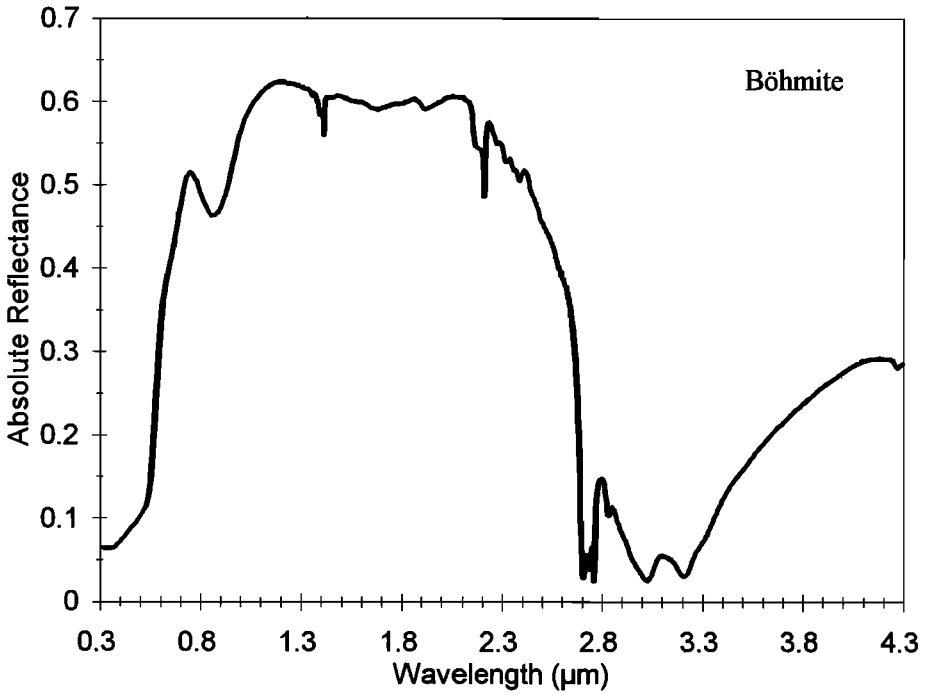

Figure 2. Plot of 0.3-4.3 μm reflectance spectrum of <45 μm size fraction of böhmite OOH005.

consist of two overlapping bands with minima at 1.82 and 1.83 μm. This feature was attributed to a combination of the 2.76 μm O-H stretching mode and the second overtone of a fundamental O-H bending mode [*Hunt et al.*, 1971]. However the sample used to make this assignment was not pure diaspore as noted by the authors and as evidenced by other spectral features not consistent with the spectra of Figure 3. A 2.76 μm band is not found in our diaspore spectra or those of other investigators for either synthetic or natural diaspore [*Rudnitskaya and Ziborova*, 1967; *Tsuchida and Kodaira*, 1990] and hence is probably attributable to these accessory phases, which Hunt et al. identify as gibbsite and kaolinite. The 1.8 μm absorption feature is probably attributable to a combination or overtone of the O-H stretching bands at 3.33 and 3.41 μm (Table 7) or some other combination involving bands near 4.7 and 5.0 μm whose assignment is uncertain [*Kolesova and Ryskin*, 1962].

The diaspore spectra also exhibit a series of generally unresolvable

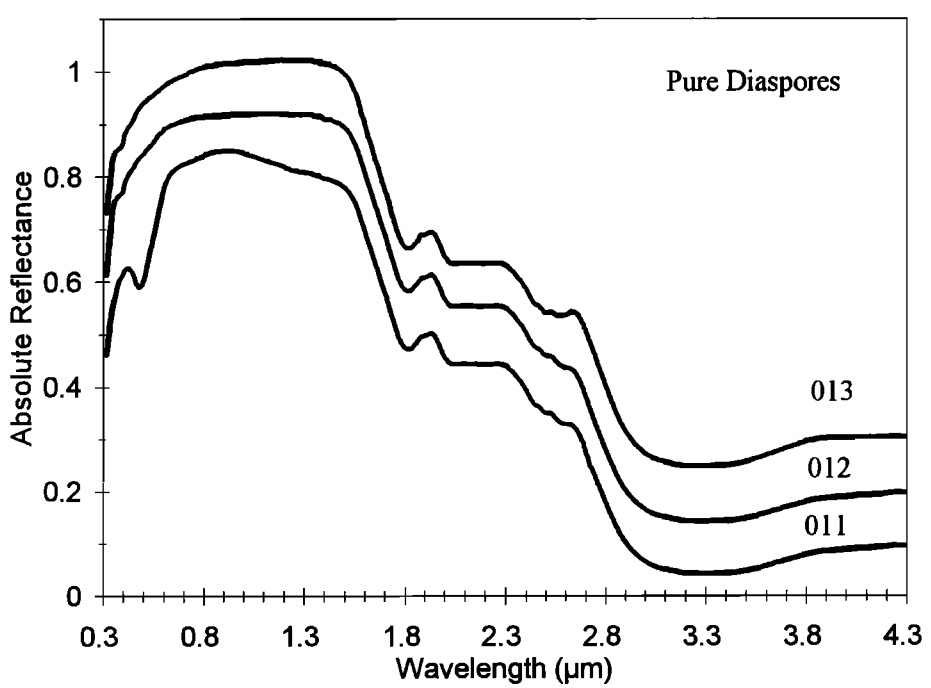

Figure 3. Plot of 0.3-4.3 μm reflectance spectra of <45 μm size fractions of pure diaspores OOH011, 012, and 013. The spectra have been vertically offset for clarity as follows: OOH012, +0.1; OOH013, +0.2.

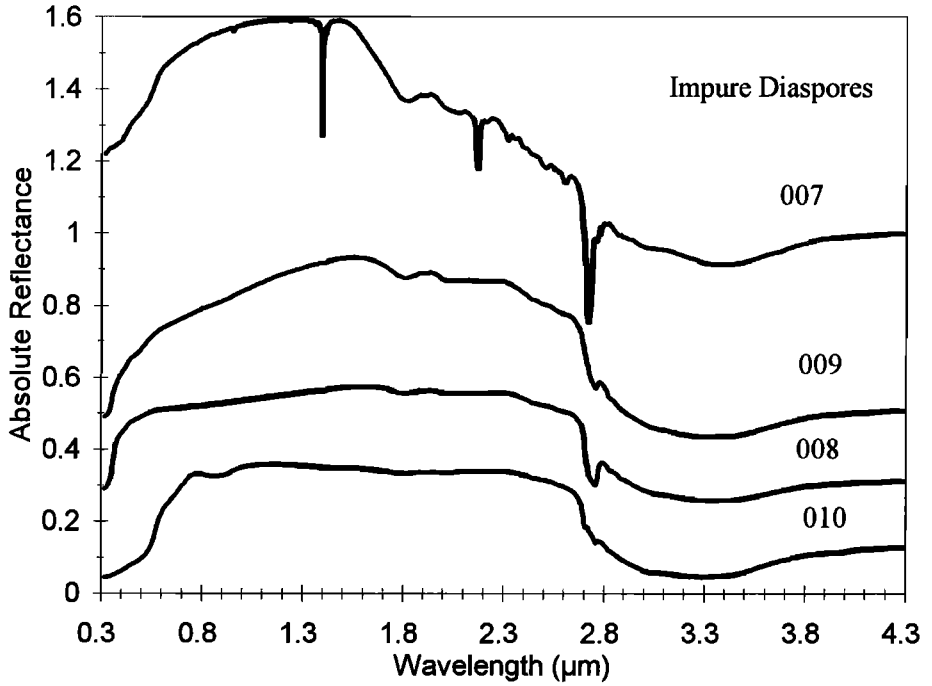

Figure 4. Plot of 0.3-4.3 μm reflectance spectra of <45 μm size fractions of impure diaspores OOH007, 008, 009, and 010. The spectra have been vertically offset for clarity as follows: OOH008, +0.2; OOH009, 0.4; OOH007, 0.7.

Table 5. Wavelength Positions of O-H Stretching Fundamental Absorption Bands Seen in Transmission Spectra of Diaspores and Diaspore-Rich Samples

Band Positions					
cm^{-1}	μm	cm^{-1}	μm	Sample Description	References
3000	3.33	2910	3.44	diaspore ore	1
3000	3.33			synthetic diaspore, other band(s)unresolved	1
2985	3.35	2924	3.42	pure synthetic diaspore	2
		2924	3.42	pure natural diaspore*	2
		2924	3.42	diaspore clay*	2
		2924	3.42	diaspore clay*	2
		2924	3.42	diaspore clay*	2
2994	3.34	2915	3.43	natural diaspore	3
3005	3.33	2927	3.42	synthetic diaspore	3
		2863	3.49	natural diaspore	4
3100	3.23	2900	3.45	natural diaspore, band positions are approximate	5
		2925	3.42	natural diaspore, spectrum not published	6
3000	3.33	2825	3.54	natural diaspore, spectrum not published	7
		2874	3.48	natural diaspore, spectrum not published	8
			~3.4	diaspore, synthetic	9
2984	3.35	2920	3.42	natural diaspore (Chester, Pennsylvania)	10
3000	3.33	2920	3.42	natural diaspore OOH007	10
3000	3.33	2922	3.42	natural diaspore OOH008	10
2998	3.34	2921	3.42	natural diaspore OOH009	10
2994	3.34	2921	3.42	natural diaspore OOH010	10
2999	3.33	2917	3.43	natural diaspore (manganoan) OOH011	10
3000	3.33	2918	3.43	natural diaspore OOH012	10
2995	3.34	2918	3.43	natural diaspore OOH013	10

References are 1, *Tsuchida and Kodaira* [1990]; 2, *Frederickson* [1954]; 3, *Kolesova and Ryskin* [1962]; 4, *Schwarzmann* [1962]; 5, *Rudnitskaya and Ziborova* [1967]; 6, *Cabannes-Ott* [1957]; 7, *Moenke* [1962]; 8, *Hartert and Glemser* [1956]; 9, *Glemser and Hartert* [1953]; 10, this study.

* Two resolvable bands seen, wavelength position of lower wavelength band unknown due to limitations in published data.

absorption features between 1.95 and 2.65 μm which result in an overall decrease in reflectance toward longer wavelengths. These can also be attributed to various combinations of the Al-O vibration and/or O-H bending and stretching fundamentals (Table 7).

The asymmetry of the O-H-O bond results in two discrete absorption bands due to O-H stretching. These bands are located near 3.33 and 3.41 μm in the reflectance spectra. The energies and separations of these bands accord well with the structure of diaspore [*Hartert and Glemser*, 1956; *Cabannes-Ott*, 1957; *Kolesova and Ryskin*, 1962; *Schwarzmann*, 1962; *Ryskin*, 1974]. These two bands are invariably present in transmission spectra but are not always apparent in reflectance spectra of the diaspore-rich samples. This is attributed to

Table 6. Wavelength Positions of Minimum Reflectance of O-H Stretching Fundamental Absorption Bands in Diaspore Reflectance Spectra

Band Positions, μm	Sample ID and Grain Size Fraction
~3.30, ~3.40	OOH007, 45-90 μm
3.34, 3.41	OOH007, <45 μm
~3.23, ~3.35, ~3.40	OOH008, 45-90 μm
3.33, 3.40	OOH008, <45 μm
~3.34, 3.41	OOH008, <5 μm
~3.19, ~3.38	OOH009, 45-90 μm
3.33, 3.41	OOH009, <45 μm
3.38, 3.41	OOH009, <5 μm
3.21, ~3.33*, ~3.46*	OOH010, 45-90 μm
~3.30	OOH010, <45 μm (manganoan diaspore)
~3.14, ~3.37, ~3.41*	OOH011, 45-90 μm
~3.30, ~3.41*	OOH011, <45 μm
~3.37, 3.43	OOH012, 45-90 μm
~3.30, ~3.40*	OOH012, <45 μm
~3.30, 3.41*	OOH012, <5 μm
~3.36, ~3.41*	OOH013, 45-90 μm
3.27, 3.32, ~3.41*	OOH013, <45 μm
3.30, ~3.33, ~3.41*	OOH013, <5 μm

* Inflection point.

Table 7. Assignments of Resolvable Absorption Features in Diaspore Spectra

Position		
cm^{-1}	μm	Assignment
520	19.2	bending vibration, precise identity unknown
575	17.4	bending vibration, precise identity unknown
675	14.8	nonplanar O-H bending vibration (γ(OH))
755	13.2	Al-O vibration
965	10.4	planar O-H bending vibration (δ(OH))
1075	9.30	planar O-H bending vibration (δ(OH))
1985	5.04	bending overtone/combination? Precise identity unknown
2110	4 74	bending overtone/combination? Precise identity unknown
2930	3.41	O-H stretching vibration
3000	3.33	O-H stretching vibration
5464	1.83	O-H stretching vibration combination/overtone (?)
5495	1.82	O-H stretching vibration combination/overtone (?)

the fact that absorption bands are invariably wider in reflectance spectra and that the intense nature of these bands results in low overall reflectance in the wavelength region of interest. The double band structure in this region is more apparent in the transmission spectra (Figure 5) and the spectrum of sample OOH007 which contains abundant pyrophyllite (Figure 6). The wavelength positions of these two bands are unique among metal hydroxides; this is related to the fact that oxygen-hydrogen bond length is negatively correlated with wavelength position of the corresponding O-H stretching fundamental band [*Schwarzmann*, 1962].

With decreasing temperature (from 300 K to 100 K) the O-H stretching bands move to shorter wavelengths [*Ryskin*, 1974]. In transmission, these bands shift from 3.345 and 3.422 μm at 300 K to 3.330 and 3.413 μm at 100 K. This shift may be used to account for small differences in band positions between room temperature laboratory spectra and spectra of extraterrestrial targets such as Mars. The presence of iron, which can partially substitute for aluminum, also affects the longer wavelength bands of diaspore (>8 μm); the corresponding effect on the shorter wavelength bands is unknown [*Caillère and Pobeguin*, 1966].

The spectra of the diaspore-rich samples (OOH007-010; Figure 4) display many of the features found in the pure diaspore sample spectra. The 1.8 μm band is evident in all cases (although greatly reduced in intensity in the OOH007 spectrum), as is the O-H stretching feature in the 3.3-3.4 μm region, although this feature is generally not resolvable into two distinct bands in reflectance. The OOH007 sample contains approximately equal amounts of pyrophyllite and diaspore and its spectrum exhibits features attributable to both phases [*Crowley*, 1984]. The presence of accessory phases, particularly hematite, is probably the main cause of the lower overall reflectance of the other samples and the reflectance decrease toward shorter wavelengths. These spectra also exhibit the more "conventional" OH absorption band in the 2.7-2.8 μm region which is not characteristic of diaspore but is consistent with the accessory phases present in these samples, such as kaolinite and other hydrated silicates. Diaspore spectral features are also evident in transmission spectra of other diaspore-rich bauxite ores [*Sijarić et al.*, 1976]

The most characteristic spectral features of diaspore are the two absorption bands located near 3.33 and 3.41 μm, which are related to the unique structural elements of this mineral. Some of the other bands, which are also quite distinctive (such as the 1.8 μm band), are weaker and hence could more readily be "masked" by accessory phases.

In order to address the possibility of detecting diaspore on the surface of Mars using reflectance spectroscopy, a number of diaspore+pyroxene and diaspore+palagonite mixtures were spectrally characterized. Reflectance spectra of a relatively unaltered orthopyroxene, diaspore OOH013, and intimate mixtures of 95% orthopyroxene + 5% diaspore OOH013, and 75% orthopyroxene + 25% diaspore OOH013 (all <45 μm grain size) are shown in Figure 7. It is worth noting how the presence of even small amounts of diaspore can drastically lower the reflectance of the pyroxene in the 3 to 4 μm

Table 8. Wavelength Positions of O-H Stretching Fundamental Absorption Bands and Various Combinations and Overtones for Goethite

Band Positions, μm	Sample Type	Spectral Type*	References
	O-H Bending Fundamentals		
10.7, 11.8			
	O-H Stretching Fundamentals		
3.18	goethite, synthetic	T	1
3 20	bauxites	T	2
3 28	goethite, natural	T	3
3 20, 3.23	goethite, natural	T	4
~2.9, ~3.2	goethite, synthetic	T	5
~3 3	goethite, synthetic	T	6
~2 9, ~3 2	goethites, synthetic	T	7
2 865	goethite, synthetic	T	8
3.231	goethite, natural	T	9
2.924, 3 003, 3.125	goethite, natural	T	10
3.125-3 190	goethite, synthetic, Al bearing	T	11
3.155	goethite, natural	R	12
2 834, 2.884, 3 242	OOH003	T	13
~3.17	OOH003, <45 μm	R	13
~3.11	OOH003, 45-90 μm	R	13
	Main Fe^{3+} Electronic Transition Bands		
~0 9	goethite, natural, <5 μm	R	14
0.64, 0.93	goethite	R	15
~0 69, ~0.88	goethite, natural, -40 mesh	R	16
~0.93	goethite, natural, solid	R	16
~0.93	goethite, α-1	R	17
~0.93	goethite, α-4	R	17
~0.91	goethite, α-2, natural	R	17
~0 65, 0.899	goethite, synthetic (GTCPS3)	R	18
~0 65, ~0 94	goethite, natural (7C)	R	18
0 6-0.66, 0.910-0.945	Mn-bearing goethites, synthetic	R	19
~0.632, ~0.920	Cr-bearing goethites, synthetic	R	20
0.645-0.652, 0.896-0.932	goethites, synthetic	R	21
0 649, 0.917	goethite, synthetic	R	22
~0.64, ~0.91	goethite, natural	R	23

Combination/Overtone Bands Position, μm	Assignment
2.42	O-H bending + O-H stretching fundamental
2.50	O-H bending + O-H stretching fundamental

References are 1, *Cambier* [1986]; 2, *Jónás and Solymár* [1970]; 3, *Hartert and Glemser* [1956]; 4, *Cabannes-Ott* [1957]; 5, *Fujita and Takahashi* [1969]; 6, *Glemser and Hartert* [1953]; 7, *Nobuoka* [1965]; 8, *Sato et al.* [1969]; 9, *Schwarzmann* [1962]; 10, *Vlasov et al.* [1970]; 11, *Wolska and Schwertmann* [1993]; 12, *Miyamoto* [1988]; 13, this study; 14, *Hunt et al.* [1971]; 15, *Geerken and Kaufmann* [1989]; 16, *Sagan et al.* [1965]; 17, *Sherman et al.* [1982]; 18, *Townsend* [1987]; 19, *Vempati et al.* [1995]; 20, *Vempati et al.* [1992]; 21, *Morris et al.* [1985]; 22, *Sherman and Waite* [1985]; 23, *Grove et al.* [1992].

*R, reflectance spectral data; T, transmission spectral data.

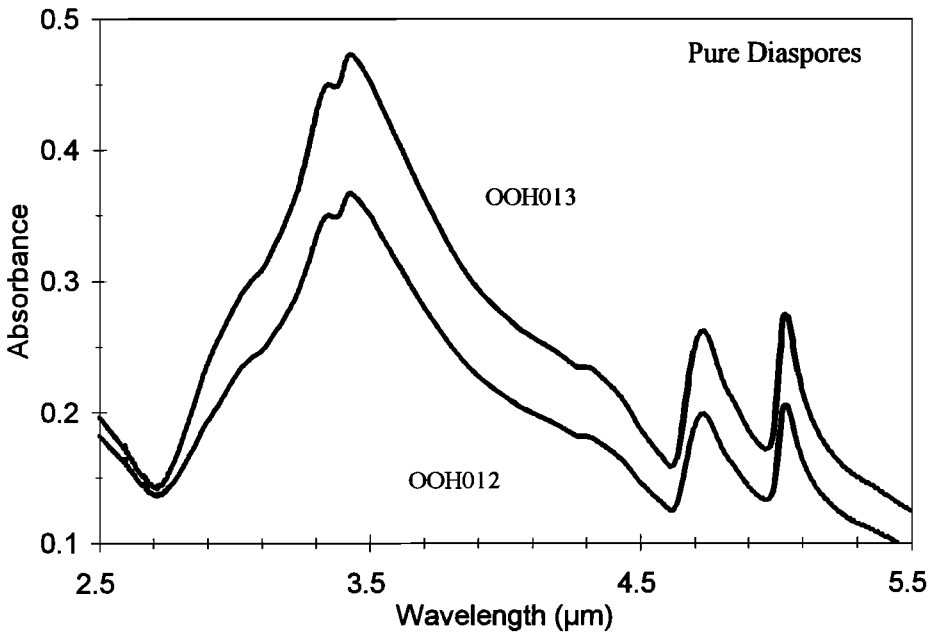

Figure 5. Infrared transmission spectra of <45 μm size fractions of diaspores OOH012 and OOH013 dispersed in KBr pellets (~1% diaspore in KBr) highlighting the two OH stretching fundamental bands.

region making this region appear very similar to pure diaspore. When the 3 to 4 μm region of the two mixture spectra are viewed in detail (Figure 8), the double band structure of the diaspore fundamental O-H stretching bands become apparent. These results suggest that the 1.8 μm band, in conjunction with the 3.33 and 3.41 μm bands, can be used to detect the presence of diaspore across a wide range of abundances.

3.4. Goethite (α-FeO(OH))

Goethite is isomorphous with diaspore [*Deer et al.*, 1962]. The spectral properties of goethite have been extensively studied by a number of investigators because of its ubiquitous occurrence in terrestrial soils and weathering environments [e.g., *Carroll*, 1970; *Kämpf and Schwertmann*, 1983; *Nahon*, 1986] and its possible presence on Mars [e.g., *Morris et al.*, 1985; *Bishop et al.*, 1993; *Geissler et al.*, 1993; *Murchie et al.*, 1993; *Cornell and Schwertmann*, 1997; *Kirkland and Herr*, 1998]. The visible and near-infrared spectra are characterized by a rise in reflectance near 0.55 μm, a sometimes resolvable absorption band near 0.65 μm and a stronger band between ~0.9 and 0.94 μm (Figure 9; Table 8), all attributable to Fe^{+3} crystal field transitions [e.g., *Mao and Bell*, 1974; *Sherman et al.*, 1982; *Morris et al.*, 1985]. The goethite spectra also exhibit two weak bands near 2.42 and 2.50 μm. These are attributable to a combination of the O-H stretching and O-H bending fundamentals (Table 8).

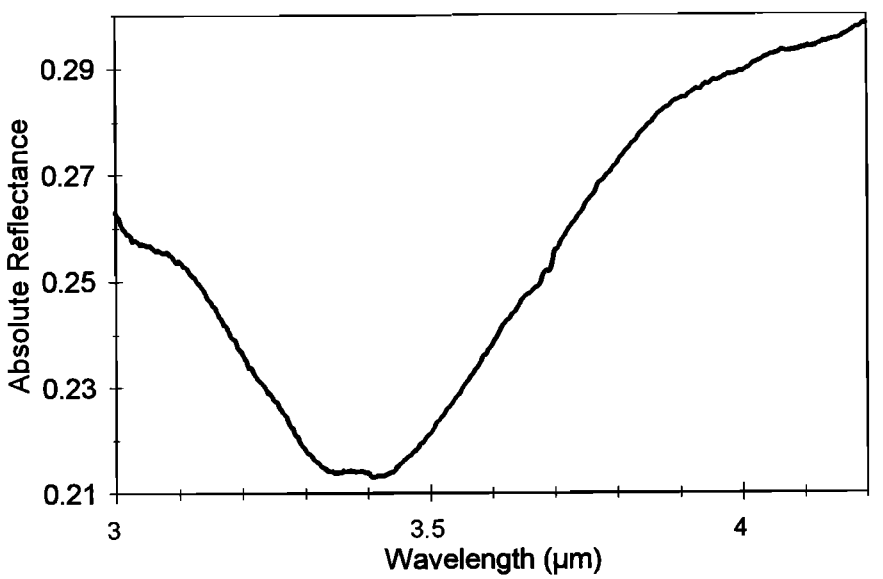

Figure 6. Plot of 3.0-4.2 μm reflectance spectrum of the <45 μm size fraction of sample OOH007 which contains approximately equal amounts of diaspore and pyrophyllite.

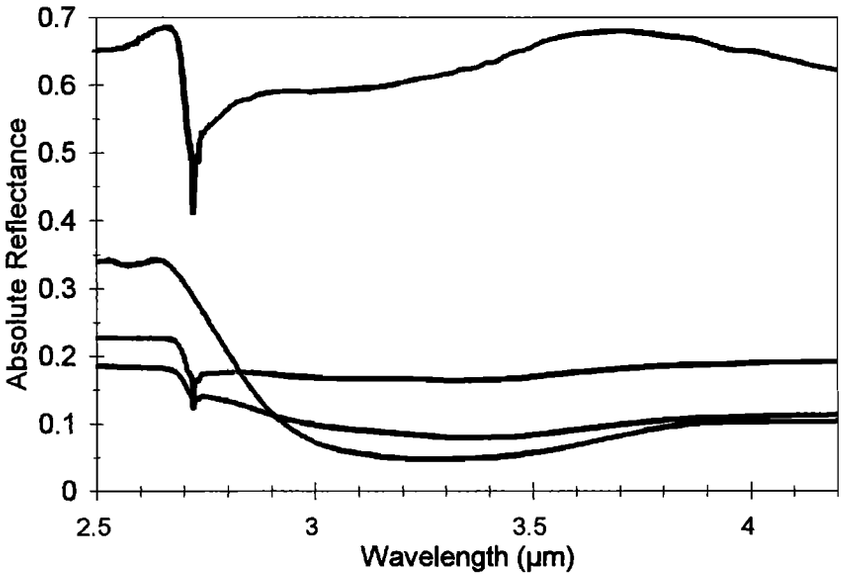

Figure 7. Plot of 2.5-4.2 μm reflectance spectra of a pure orthopyroxene (PYX110), a pure diaspore (OOH013), and intimate mixtures of 95% PYX110 + 5% OOH013, and 75% PYX110 + 25% OOH013. All samples are <45 μm grain size. The curves decrease in reflectance at 3.3 μm in the series PYX110, 95/5 mixture, 75/25 mixture, OOH013.

At longer wavelengths, goethite exhibits a broad absorption feature between 3.1 and 3.3 μm attributable to O-H stretching vibrations (Table 8); it is sometimes resolvable into two closely spaced absorption bands, analogous to the situation for diaspore but with a smaller separation between the bands [*Cambier*, 1986]. Band position variations between different studies are probably attributable to some combination of spectral resolution (which prevents clear resolution of the two overlapping absorption bands), quality of the published spectra, possibly small variations in structure and degree of crystallinity between different samples, and effects of adjacent absorption bands due to OH in accessory phases. The latter explanation probably accounts for the differences seen in the position of the O-H stretching fundamental band in the spectra of the two size fractions of sample OOH003 (Figure 9).

Due to the isomorphous nature of goethite and diaspore, a number of investigators have examined the issue of Al-Fe substitutions between the end members. It has been found that complete solid solution between these end members cannot be achieved in the laboratory and is not found in nature [*Norrish and Taylor*, 1961; *Caillère and Pobeguin*, 1966; *Wefers*, 1967a, b; *Jónás and Solymár*, 1970; *Solymár and Jónás*, 1971; *Wolska and Schwertmann*, 1993]. These studies indicate that this miscibility gap is due to the fact that the

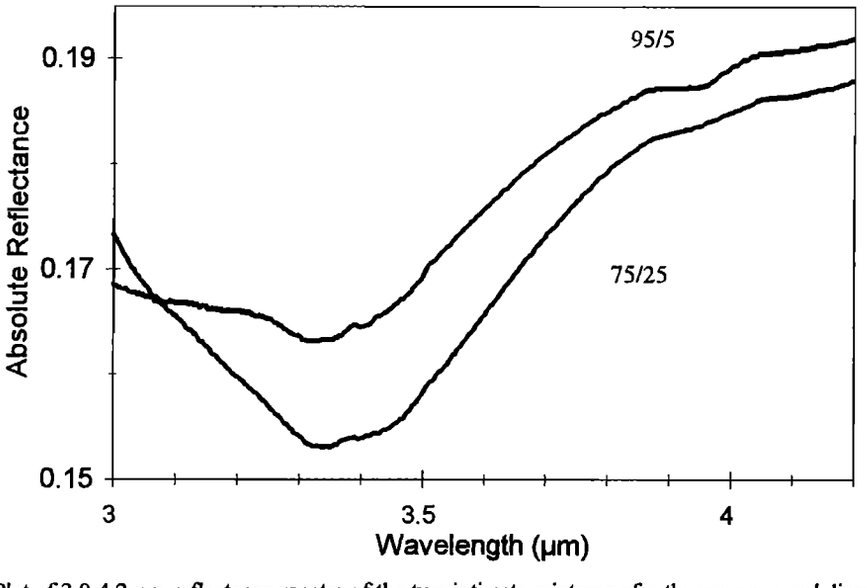

Figure 8. Plot of 3.0-4.2 μm reflectance spectra of the two intimate mixtures of orthopyroxene and diaspore shown in Figure 7 (95/5 and 75/25). The 75/25 mixture has been vertically offset by +0.075.

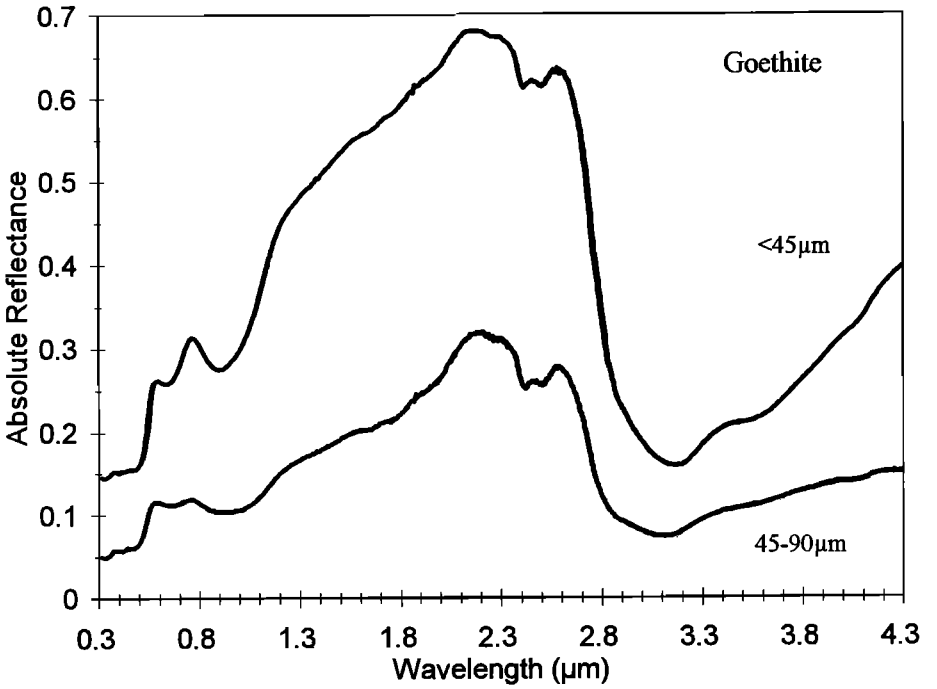

Figure 9. Plot of 0.3-4.3 μm reflectance spectra of <45 and 45-90 μm size fractions of goethite (OOH003). The <45 μm size fraction spectrum has been offset +0.1 for clarity.

mechanism of substitution is complex. The substitutions that occur do affect the positions of the O-H fundamental bands in the spectra [*Caillère and Pobeguin*, 1966].

3.5. Manganite (MnO(OH))

Manganite has a similar formula to diaspore and goethite but is not isostructural with them [*Kostov*, 1968]. However, it is much more common in nature than the isostructural form of α-MnO(OH), groutite [*Deer et al.*, 1962]. The spectral properties of manganite have not been intensively studied. The manganite spectrum (Figure 10) is characterized by a rise in reflectance in the 0.8 μm region and absorption features near 1.97 μm and 2.3 μm which are probably attributable to O-H stretching and bending combinations, and perhaps an Mn-O + O-H combination, respectively (Table 9). However, the

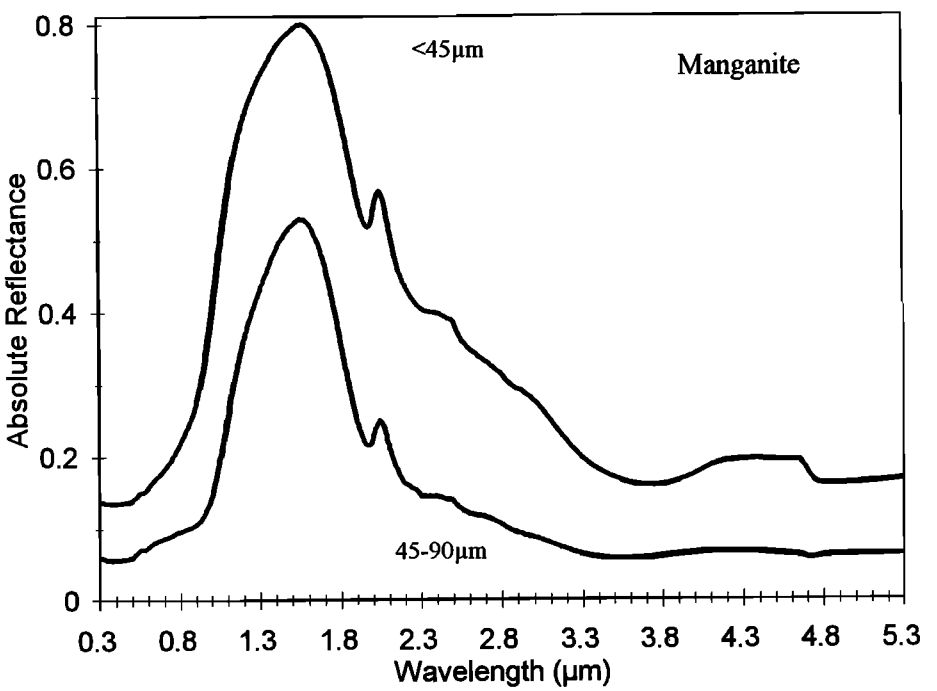

Figure 10. Plot of 0.3-5.3 μm reflectance spectra of <45 and 45-90 μm size fractions of manganite (OOH006). The <45 μm size fraction spectrum has been offset +0.1 for clarity.

Table 9. Wavelength Positions of O-H Stretching Fundamental Absorption Bands and Various Combinations and Overtones for Manganite

Band Positions, μm	Sample Type	Spectral Type*	References
	O-H Bending Fundamentals		
8.7, 9 0, 9.3			1, 2
	O-H Stretching Fundamentals		
3.810, 4.902	manganite, natural	T	1
3.816, 4.932	OOH006	T	3
~3.75, ~4.89	OOH006, <45 μm	R	3
~3.59, 4.725	OOH006, 45-90 μm	R	3

Combination/Overtone Bands Position, μm	Assignment
1.97	combination or overtone of O-H stretching fundamentals
2.3	combination of Mn-O and O-H stretch (?)

References are 1, *Cabannes-Ott* [1957]; 2, *Ryskin* [1974]; 3, this study.
*R, reflectance spectral data; T, transmission spectral data.

far-infrared absorption bands of manganite are not well characterized, and the latter assignment is based on spectral similarities with other metal hydroxides [*Hunt and Salisbury,* 1970; *Hunt et al.,* 1971; *Hunt,* 1979]. Absorption features analogous to the Mn^{3+} electronic transitions near 0.45 and 0.6 μm found in Mn-substituted goethites [*Vempati et al.,* 1995] are probably present but not readily apparent due to the low overall reflectance in this region. Such features may be attributable to Mn^{2+} transitions.

At longer wavelengths, two bands due to O-H stretching are found, near 3.8 and 4.9 μm (Table 9). These bands are equivalent to the two O-H stretching bands of goethite and diaspore but with a much larger separation due to the more distorted crystal structure of manganite [*Cabannes-Ott,* 1957]. The differences in band minima positions between the two grain sizes are probably attributable to the low overall reflectance, which suggests that these bands are saturated in the larger grain size and/or small amounts of accessory phases are present which are not apparent in the XRD data.

4. Discussion

The aluminum hydroxides and other metal hydroxides related to diaspore exhibit a wide range of spectral properties. The variations are a function of both structural differences between the various hydroxides as well as differences in cation radii [*Schwarzmann,* 1962]. The wavelength position of the various O-H stretching fundamentals are different between the various aluminum hydroxides (Table 10), as expected from a consideration of their structural (bond length) differences. The spectral effects of different cations in otherwise isostructural hydroxide minerals can be gauged from a comparison of the goethite and diaspore spectra. These two minerals are generally considered to be isostructural, although the fact that Fe and Al cations are of different sizes leads to incomplete solid solution between these end members, complex coupled substitutions, and slight differences in structural properties of the end members themselves [*Cabannes-Ott,* 1957; *Schwarzmann,* 1962; *Caillère and Pobeguin,* 1966; *Jónás and Solymár,* 1970; *Károly and Klára,* 1971; *Wolska and Schwertmann,* 1993]. These differences account for differences in overall reflectance, the appearance of absorption features associated with the cations, and variations in wavelength positions of the O-H stretching fundamentals (~3.20 and ~3.23 μm in goethite versus 3.33 and 3.41 μm in diaspore; Table 10).

Structural differences between compositionally identical end members are also expressed in reflectance spectra. Diaspore and böhmite are both composed of AlOOH but are structurally different. This leads to changes in O-H bond lengths which result in the fundamental O-H stretching bands appearing at different wavelength positions (3.03 and 3.21 μm in böhmite versus 3.33 and 3.41 μm in diaspore; Table 10). These results indicate that high-quality, high spectral resolution spectra acquired in the 3-4 μm wavelength region can be used to discriminate a wide range of metal hydroxides, including isostructural minerals.

The diaspore spectra, which are the focus of this study, are unique in a number of respects. The position of the absorption feature near 1.8 μm, which is attributable to overtones and/or combinations of the O-H stretching fundamentals, differs from most other OH-bearing minerals which generally exhibit such features closer to 1.9 μm [*Hunt,* 1979]. Similarly, diaspore is the only (nonorganic) mineral examined which displays two absorption bands in the 3.3-3.5 μm region [*Silverstein et al.,* 1991]. Thus the appearance of two bands near 3.33 and 3.41 μm is uniquely attributable to this mineral if both bands are assumed to be due to a single phase.

Comparison of the pure diaspore and diaspore-rich spectra provides some insights into the spectral detectability of diaspore. The diaspore-rich spectra exhibit wide variations in spectral properties below 1.5 μm (Figure 4). These variations include differences in overall spectral shape, slope, and appearance of absorption features; all are largely attributable to the presence of hematite which has been found to have a very profound effect on reflectance spectra at wavelengths below approximately 1.5 μm [*Sherman et al.,* 1982; *Morris et al.,* 1985]. This is confirmed by the fact that longer wavelength bands such as the 1.8 μm diaspore band are present in all of the diaspore-rich sample spectra. The longer wavelength O-H stretching fundamental bands (3.33 and 3.41 μm) are also apparent in all of these spectra and their positions do not vary appreciably from those of the pure diaspores. This suggests that the presence of diaspore is most readily deduced from the presence of the two O-H fundamental stretching bands near 3.33 and 3.41 μm, although these bands can become saturated with increasing diaspore content, resulting in a broad unresolved absorption feature. The 1.8 μm feature is less intense and may be resolvable depending on the signal-to-noise ratio of the data and the nature and abundance of any accessory phases.

Attempts to model the spectral detection limits for diaspore in mixtures, for application to spectroscopic studies of Mars, are hampered by the fact that detection limits are a function of the optical properties, grain sizes, and abundances of additional phases that are present [e.g., *Sabol et al.,* 1992]. The reflectance and transmittance spectra indicate that resolution of the fundamental O-H stretching

Table 10. Summary of Wavelength Positions of O-H Stretching Fundamental Absorption Bands

Mineral	Band Positions, μm
Gibbsite	2.76, 2.82, 2.88, 2.94, 2.96
Böhmite	3.03, 3.23
Diaspore	3.33, 3.41
Goethite	3.20*, 3.23*
Manganite	3.8, 4.9

*Normally expressed as an unresolved double band.

bands in diaspores is enhanced by dispersion of the diaspore in a spectrally "neutral" medium; in pyrophyllite in the case of sample OOH007 (Figure 4), in KBr for transmission measurements (Figure 5), or in orthopyroxene (Figure 8). In addition, the presence of iron hydroxides does not appear to appreciably affect the ability to discriminate the diaspore O-H stretching fundamental bands

It appears that different metal hydroxides, particularly diaspore, possess sufficient spectral uniqueness to permit their identification in reflectance spectra. When coupled with the fact that these minerals form under a variety of restrictive conditions (see below), spectral detection of specific metal hydroxides enables constraints to be placed on geological histories of targets.

Diaspore is currently not a major aluminum ore because other aluminum hydroxides, such as böhmite and gibbsite, are more easily processed. Diaspore requires more aggressive treatments (such as higher temperatures) than other aluminum hydroxides to extract the metal. This processing consideration translates into enhanced stability of diaspore relative to other aluminum hydroxides which has implications for its survival on the surface of Mars as discussed below.

5. Formation Conditions and Stability of Diaspore

Surficial deposits of Al hydroxides are widespread across the Earth's surface [e.g., *Jacob*, 1984]. Bauxite deposits (defined as those deposits containing >50% oxides and hydroxides of Al, Fe, and Ti, with Al minerals being more abundant than the minerals of the other two elements combined) normally contain one or more of gibbsite, böhmite, and diaspore as the main Al hydroxides [e.g., *Bárdossy and Aleva*, 1990]. Diaspore is found in a great number of deposits which are otherwise composed almost entirely of the other two main Al hydroxides, in abundances up to 4% [*Bárdossy and Aleva*, 1990]. The most important factors that seem to affect the formation of bauxite include climate, pH and Eh of percolating water, the amount of percolating water, rate of percolation, temperature, composition, and permeability of the host and precursor rocks, and topography. The Al hydroxides are invariably concentrated in the uppermost layers of a deposit, due to the fact that they are a residual weathering product, and leaching and percolation of rainwater operate most effectively at the Earth's surface.

The most important common characteristic of bauxite deposits which promotes the formation of Al hydroxides include a subtropical climate with abundant rainfall (with or without monsoon conditions) [*Abbott*, 1958]. Formation of Al hydroxides proceeds via hydrolysis and/or dissolution and leaching/removal by circulating water of progressively less mobile elements [*Bárdossy and Aleva*, 1990]. Thus any rock which contains aluminum can potentially be converted, in situ, to an aluminum hydroxide-rich deposit. In cases where rapid and intense percolation by (rain)water occurs (e.g., some areas of Kauai), such as in fractured or vesicular basalts, aluminum may be mobilized and transported downward over a short distance to be precipitated as Al hydroxides [*Abbott*, 1958; *Bates*, 1960].

The pH and Eh of circulating fluids will affect the order in which elements are dissolved as well as the relative rates of dissolution. After titanium, aluminum is the least mobile of the common rock-forming elements, when exposed to water with a pH of between ~4 and ~9 [e.g., *Jacob*, 1984; *Siever and Woodford*, 1979]. Hydrolysis of basic rocks, which tends to increase the pH of percolating water, can be moderated by the presence of dissolved carbon dioxide [*Keller*, 1964]. CO_2-rich water also seems to promote the formation of diaspore over gibbsite [*Allen*, 1935]. Small changes in Eh will trigger the formation of either diaspore or böhmite or both at the same time [*Bárdossy*, 1982].

Water is necessary for effecting hydrolysis of anhydrous minerals prior to dissolution and for transporting dissolved elements away from the site of dissolution. A high degree of permeability and intense and sustained percolation by water are also necessary for removing mobilized elements from the site of dissolution prior to their reprecipitation [*Keller*, 1964]. The most aluminum hydroxide-rich parts of a bauxite deposit are commonly found in the areas of most intense groundwater percolation; these are also the zones which are frequently enriched in diaspore relative to the other Al hydroxides [*Bárdossy*, 1982; *Keller and Stevens*, 1983]. Diaspore is often found in the highest concentrations in deposits which have experienced the most desilication; these zones again corresponding to areas with the best drainage and hence most intense percolation [*Nia*, 1968, 1969; *Bárdossy*, 1982; *Keller and Stevens*, 1983]. Given the fact that bauxite formation is a surface weathering process, the source of the water is precipitation in liquid form (i.e., rain).

Formation of aluminum hydroxides in colder, more arid, or glacial/periglacial environments would be hampered by two main factors: low temperatures and/or the paucity of liquid water. Liquid water is required to permit sufficient percolation, leaching, and transport of dissolved ions. Low temperatures also result in lower dissolution rates for all rock types except carbonates. In such environments physical weathering dominates over chemical weathering [*Ugolini*, 1986]. Consequently, neither bauxite/laterite formation nor deposits have been found in environments which do not currently possess, or which possessed in the past, tropical environments (abundant rainfall, warm temperatures) [e.g., *Bárdossy*, 1982; *Bárdossy and Aleva*, 1990].

The formation of Al monohydrates such as diaspore and böhmite from Al trihydrates such as gibbsite is dependent on the vapor pressure of water, with low pressures favoring the former phases [*Kennedy*, 1959; *Wayman*, 1963]. Diaspore has also been found to form directly from the breakdown of clay minerals [*Allen*, 1935; *Kennedy*, 1959] as well as from the dehydroxylation of böhmite in areas with "optimum" drainage [*Valeton*, 1972] and conversion from gibbsite [*Allen*, 1935]. Increasing temperature also results in increasing rates of dissolution of most elements, but this is not a necessary condition if enough time is available for percolation and leaching to occur. The conditions which seem to favor diaspore formation, versus other Al hydroxides, are parental kaolinite, and continuous hydrolysis without periods of drying [*Keller et al.*, 1954].

Topography also plays a role in bauxite formation. Relatively flat land will be more conducive to percolation than steep slopes. Positive landforms (plateaus) with gentle slopes are required to promote percolation over runoff and avoid the reprecipitation of dissolved elements within the uppermost weathering profile [e.g., *Bárdossy and Aleva*, 1990]. Given suitable conditions, meter-thick bauxite weathering profiles can develop in less than 1 million years [*Bárdossy and Aleva*, 1990].

In the case of basalts, mafic, and ultramafic rocks, feldspars and aluminum-bearing pyroxenes can weather, ultimately, to aluminum hydroxides. Field observations and laboratory experiments show that the general sequence of events in the weathering of basalts is to progressively simpler compositions which are also progressively enriched in aluminum. Thus a common weathering sequence is basalt

to montmorillonite type clays to kaolinite to aluminum hydroxides. Each mineral formed during intermediate stages can be weathered to the next stage by percolation of water across a wide range of pH values (~4-9). This sequence of weathering has been observed in numerous basaltic, mafic, and ultramafic sequences and in laboratory studies [e.g., *Seelye et al.*, 1938; *Hanlon*, 1944; *Sherman*, 1949; *Carroll and Woof*, 1951; *Jackson et al.*, 1952; *Butler*, 1954; *Millot and Bonifas*, 1955; *Sherman and Uehara*, 1956; *Tiller*, 1958; *Sherman and Ikawa*, 1959; *Correns*, 1961; *Coleman*, 1962; *Loughnan*, 1962; *Carroll and Hathaway*, 1963; *Keller*, 1964; *Valeton*, 1972; *Brigatti*, 1983; *Carroll*, 1970; *Maksimović*, 1976; *Siever and Woodford*, 1979; *Nahon and Colin*, 1982; *Nahon et al.*, 1982; *Kodama et al.*, 1988]. When volcanic glass or tuff is the parent rock, palagonite is commonly the intermediate weathering product [*Bates*, 1962; *Hay and Iijima*, 1968]. Weathering is also enhanced in tuffs as opposed to more compact basalts or andesites [*Carroll and Hathaway*, 1963].

While the conditions required to form Al hydroxides are well understood, the phase relationships among the different minerals in this group (gibbsite, böhmite, and diaspore) are somewhat uncertain, largely due to the slow kinetics of transformation at Earth surface temperatures and pressures. Measurable conversions are generally not reproducible in the laboratory without the use of seed crystals [e.g., *Valeton*, 1972].

Diaspore was long thought to require elevated temperatures and/or pressures for its formation. However, it has been shown that diaspore is the stable phase across a wide temperature range. On the high-temperature side, it is stable up to ~370°C whereupon it dehydroxylates to corundum [e.g., *Stumpf et al.*, 1950; *Kennedy*, 1959; *Valeton*, 1972]. At Earth surface pressures, diaspore is stable to as low as 70°C (or less) depending on the composition of percolating solutions [e.g., *Wefers*, 1967a, b, c; *Valeton*, 1972]. Both laboratory and field investigations suggest that diaspore can form directly at Earth surface pressures and temperatures probably by minor structural rearrangements of an aluminum hydroxide framework that remains after dissolution and removal of silicon from clay mineral precursors [e.g., *Kennedy*, 1959; *Kiskyras*, 1960; *Nia*, 1969]. Some investigators have also suggested that böhmite is entirely a metastable phase and that diaspore is the only stable Al monohydrate; the presence of böhmite with or without diaspore being due to the fact that the conversion of böhmite to diaspore is exceedingly slow [*Kennedy*, 1959; *Wefers*, 1967a, b]. The existence of multiple phases in a single deposit is probably a reflection of the low rate of formation of diaspore under surface conditions and the different environments which can exist within a single deposit. It is also believed that diaspore can crystallize from amorphous precursors under Earth surface conditions, once again from the dissolution of clay minerals [*Mindszenty*, 1976].

The general observations concerning diaspore are that this mineral is most common in the oldest (Paleozoic) bauxite deposits, including those which have not been subjected to tectonic deformation and metamorphism [e.g., *Nia*, 1969]; diaspore is also widely present (generally at the 0.1-0.5% level) in younger gibbsite- and böhmite-rich deposits [*Harder*, 1949; *Bárdossy*, 1982; *Patterson et al.*, 1986; *Bárdossy and Aleva*, 1990]. This suggests that the kinetic inhibitions to diaspore formation can be overcome over geological timescales. The conversion process can be accelerated if intense percolation and leaching can be maintained, as evidenced by the fact that diaspore is commonly concentrated in the most well-drained parts of a deposit [*Kennedy*, 1959; *Bárdossy and Aleva*, 1990]. There is also some evidence that in deposits where the diaspore:böhmite ratio reaches ~1, rapid subsequent conversion of the remaining böhmite to diaspore may occur [*Nia*, 1969].

The conversion of Al trihydrates to Al monohydrates can be achieved at the surface through dehydroxylation of the former via the heating effects of solar insolation or cyclical or prolonged desiccation [*Bárdossy*, 1982; *Jacob*, 1984]. Once formed, indurated, diaspore-rich bauxite deposits are highly resistant to subsequent erosion [*Mead*, 1915; *Keller*, 1952; *Nia*, 1969; *Valeton*, 1972; *Keller and Stevens*, 1983; *Jacob*, 1984].

Diaspore formation is promoted by the presence of goethite, which is isomorphous with diaspore [*Deer et al.*, 1962]. In the presence of abundant iron, diaspore rather than böhmite formation is promoted [*Nia*, 1969]. Goethite is a low-temperature stable Fe hydroxide and commonly forms in association with Al hydroxides in bauxites [e.g., *Bárdossy*, 1982; *Bárdossy and Aleva*, 1990]. It is most commonly found in the same climatic environments which promote bauxitization [*Kämpf and Schwertmann*, 1983]. Goethite acts as a nucleating site for diaspore, accelerating the crystallization of diaspore and lowering the required temperature of formation of diaspore [*Wefers*, 1967b, c]. Goethite can subsequently be dehydroxylated to form hematite at temperatures as low as ~50°C [*Wefers*, 1967c]. Hematite (like diaspore) is more common in older bauxite deposits than goethite [e.g., *Caillère and Pobeguin*, 1964; *Bárdossy*, 1982]. While iron hydroxides are commonly found in association with Al hydroxides in bauxites, in areas where rain is persistent and percolation is intense, stable, and well developed (specifically where groundwater levels do not fluctuate), accompanying iron hydroxides may not be present [*Sherman*, 1952; *Mohr and Van Baren*, 1954].

6. Implications for Diaspore on Mars

Diaspore is a plausible candidate for comprising some portion of the Martian surface on the basis of a number of criteria. The most important requirements for its formation (described above) include an aluminum-bearing precursor, intense percolation of water, good drainage, and moderate pH.

Direct analysis of Martian surface materials indicates that aluminum is present in rocks and soils at abundances of between 7 and 10% [*Clark*, 1993; *Rieder et al.*, 1997]. Basalts, which can weather to diaspore, appear to be a widespread component of the Martian surface [e.g., *Singer et al.*, 1979; *Singer*, 1985; *Pinet and Chevrel*, 1990; *Mustard et al.*, 1993; *Mustard and Sunshine*, 1995], although the aluminum content of the unaltered basaltic materials has not yet been directly determined. Martian meteorites contain between 1 and 10% Al_2O_3 [*Banin et al.*, 1992; *McSween and Treiman*, 1998]. Thus they are all capable of weathering to Al hydroxides, since the Al content of the precursor rocks is not a major determinant in whether Al hydroxides will form [e.g., *Valeton*, 1972; *Bárdossy*, 1982; *Bárdossy and Aleva*, 1990]. The formation of palagonite, which has been suggested as being a major component of Martian dust [*Singer*, 1982; *Morris et al.*, 1989; *Soderblom*, 1992; *Bell et al.*, 1993], is often accompanied by relative enrichment of aluminum [*Geptner*, 1970; *Morris et al.*, 2000], a key requirement for diaspore formation.

As mentioned, diaspore formation is promoted by the presence of goethite and more generally by an iron-rich environment. Goethite has been tentatively identified from remote observations of Mars [*Kirkland and Herr*, 1998; *Morris and Golden*, 1998]. Hematite, which is a common weathering product of goethite, and which is commonly found in association with diaspore, also appears to be present on the

Martian surface in a wide range of crystallinity [e.g., *Morris et al.*, 1989; *Bell et al.*, 1990; *Christensen et al.*, 1999]. Less well-defined iron-bearing phases are also present across much of the surface [e.g., *Morris et al.*, 1993]. As discussed above, iron-bearing phases, such as goethite and hematite, are commonly associated with diaspore in terrestrial deposits.

Anatase (TiO_2) is a common accessory mineral in bauxite deposits due to the low mobility of titanium in weathering environments associated with terrestrial bauxite deposits [e.g., *Bárdossy and Aleva*, 1990]. Anatase has been suggested as being a possible component of Martian dust [*Pang and Ajello*, 1977], and FeTi oxides (spinels) have been suggested as being responsible for the observed magnetic properties of Martian airborne dust grains [e.g., *Coey et al.*, 1990; *Madsen et al.*, 1999; *Morris et al.*, 2000]. Titanium is present, at up to ~1% TiO_2 in Martian soil and meteorites [*Banin et al.*, 1992; *Clark*, 1993; *Rieder et al.*, 1997]. Thus the essential elements and the common accessory phases found in terrestrial diaspore deposits have either tentatively or directly been identified on Mars.

One of the most important factors in diaspore formation is intense percolation of water and good drainage. The fact that Mars is heavily cratered and likely possesses a deep megaregolith suggests that good drainage is widespread across the surface [e.g., *MacKinnon and Tanaka*, 1989; *Clifford*, 1993]. The evidence for a wetter earlier climate on Mars is currently indirect but is based on a number of persuasive geomorphological criteria such as young valley networks on the flanks of volcanoes and climatological models [e.g., *Pollack et al.*, 1987; *Postawko and Fanale*, 1993; *Squyres and Kasting*, 1994; *Carr*, 1996]. It should be noted that in the case of terrestrial bauxite deposits, rain is invariably the source of the circulating fluid [e.g., *Valeton*, 1972]. While no terrestrial diaspore deposits have been linked to formation by hydrothermal activity, this does not preclude such a connection. In the case of Mars, hydrothermal activity may be the mechanism promoting the circulation of water. The evidence for widespread heat sources on Mars and the probability of a porous regolith certainly suggest that hydrothermal formation of diaspore on Mars is possible.

Whether regimes of intense and prolonged water circulation were attained on Mars in the past is not well constrained [e.g., *Carr*, 1996]. Based on analogies with terrestrial diaspore deposits, any hydrothermal activity would need to be prolonged, relatively stable, and relatively low temperature. If diaspore did form at depth, this material would need to become exposed at the surface for detection by spectrophotometry.

One of the conditions favoring diaspore formation, through selective dissolution of more mobile elements, is a pH of between ~4 and 9 [*Bárdossy and Aleva*, 1990]. There are a number of arguments which can be invoked to increase or decrease the pH of groundwater on Mars. Simple weathering of basalts results in an increase in the pH of the water in contact with the rock [*Carroll*, 1970]. The presence of abundant CO_2 in a putative early thick Martian atmosphere would counteract this increase in pH, and the presence of sulphates and ferric-bearing assemblages in the Martian regolith suggests acidic conditions may have prevailed [e.g., *Burns and Fisher*, 1993]. Collectively, these arguments indicate that Martian groundwater pH values are not well constrained; it is also reasonable to assume that Mars was not characterized by a single global and invariant groundwater pH value. Thus there are no compelling arguments to indicate that Martian groundwater pH values would normally have been outside the range of 4 to 9. If diaspore did form on Mars it would be relatively stable against both mechanical erosion [*Mead*, 1915; *Keller*, 1952; *Nia*, 1969; *Valeton*, 1972; *Keller and Stevens*, 1983; *Jacob*, 1984] and further dehydroxylation under current Martian surface conditions [*O'Connor*, 1968].

Terrestrial diaspore deposits are widespread and many of them cover areas ranging up to tens or hundreds of square kilometers [*Bárdossy*, 1982]. If such deposits formed on Mars via similar processes and were exposed at the surface, they should be detectable in Earth-based high spatial resolution near-infrared spectra, primarily through the existence of the diagnostic bands in the 3 to 4 μm region (Table 10).

Interestingly, diaspore and other Al hydroxides would not be particularly detectable from remote sensing observations at visible or thermal infrared wavelengths, because of their relative lack of diagnostic spectral features at those wavelengths. It appears that for diaspore and other pure Al hydroxide minerals, the optimum spectral region for detectability and characterization is in the near infrared, specifically in the 3 to 4 μm region. The diaspore absorption band near 1.8 μm would only be detectable at higher diaspore abundances than the 3.33 and 3.41 μm bands. Interpretations of recent telescopic observations of Mars in the 3-4 μm wavelength region are consistent with the presence of diaspore on Mars (Bell et al., submitted manuscript, 1999) and provide perhaps the first definitive identification of the long-inferred "hydrated mineral component" on that planet's surface.

7. Summary and Conclusions

Diaspore and other simple metal hydroxides possess relatively simple reflectance spectra. The most intense and diagnostic spectral features at wavelengths below ~8 μm are due to O-H stretching fundamentals. The positions and number of these bands are unique to each type of metal hydroxide examined and thus can be used to discriminate different members of this family.

The spectral properties of diaspore, which were examined in more detail due to their possible presence on Mars, possess two intense O-H stretching fundamental absorption bands near 3.33 and 3.41 μm. Lower wavelength bands are weaker and are assigned to various overtones and combinations of fundamental bands. The O-H stretching bands are in a wavelength region accessible by Earth-based and/or Mars orbital imaging spectrometers. The presence of diaspore intimately mixed with basaltic minerals such as pyroxene, or basaltic weathering products (i.e., palagonite) should be detectable in high-quality spectra for diaspore abundances at least as low as 5 wt %.

All of the conditions which appear to promote the formation of diaspore on the Earth and which are associated with terrestrial diaspore deposits, may have existed on Mars in the past. The source of the liquid water which would have been necessary for diaspore formation on Mars cannot be uniquely determined at present, but based on the known and presumed formation conditions of terrestrial deposits, and the fact that diaspore is a surface weathering product, precipitation and/or intense subsurface percolation are the most likely source(s) of this water. Given that diaspore is a surficial weathering product formed from aluminum-bearing precursor rocks and is both mechanically and chemically resistant to further erosion, it seems likely that if diaspore did form earlier in Mars' history, such deposits would likely persist to the present time and could be areally extensive enough to be detected by near-infrared remote sensing observations.

Acknowledgments. This study was supported by the University of Winnipeg through a start-up grant and research grant through the Discretionary Grants Program (to E.A.C.) and a NASA Planetary Geology and Geophysics Program grant (to J.F.B.; NAG5-4333). We wish to extend very special thanks to George Fulford and his colleagues at the Kingston Research and Development Centre of Alcan International Limited for providing extensive analytical support and a number of the samples. Thanks also to the National Museum of Natural History of the Smithsonian Institution for providing a number of diaspore samples. Reflectance spectra were acquired at the multi-user NASA-supported Reflectance Experiment Laboratory (RELAB) facility in the Department of Geological Sciences at Brown University; we would like to acknowledge the support provided by Carle Pieters and Takahiro Hiroi for permitting access to the facility and their assistance in preparation of some of the samples for spectral measurements. Finally, our thanks to Richard Morris and an anonymous reviewer for their insightful comments which helped us to strengthen and improve this paper.

References

Abbott, A.T., Occurrence of gibbsite on the island of Kauai, Hawaiian Islands, *Econ. Geol., 53,* 842-853, 1958.

Allen, V.T., Mineral composition and origin of Missouri flint and diaspore clays, *Mem. Geol. Surv. Bienn. Rep. Appl. VI, 58,* 5-24, 1935.

Anderson, D.M., and A.R. Tice, The analysis of water in the Martian regolith, *J. Mol. Evol., 14,* 33-38, 1979.

Authier-Martin, M., G. Fulford, and F. Feret, Bauxite extractable phases in the Bayer high-temperature process: Re-assessment of boehmite content and aluminium substitution in alumino-goethite, paper presented at 5th International Alumina Quality Workshop, Worsley Alumina Pty Ltd., Bunbury, Western Australia, March 21-26, 1999.

Banin, A., B.C. Clark, and H. Wänke, Surface chemistry and mineralogy, in *Mars,* edited by H.H. Kieffer et al., pp. 594-625, Univ. of Ariz. Press, Tucson, 1992.

Bárdossy, G., *Karst Bauxites: Bauxite Deposits on Carbonate Rocks,* Elsevier Sci., New York, 1982.

Bárdossy, G., and G.J.J. Aleva, *Lateritic Bauxites,* Elsevier Sci., New York, 1990.

Bates, T.F., Rock weathering and clay formation in Hawaii, *Bull. Earth Miner. Sci. Exp. Stn. Pa. State Univ., 29,* 3-6, 1960.

Bates, T.F., Halloysite and gibbsite formation in Hawaii, in *Proceedings of the National Conference on Clays and Clay Mineralogy,* pp. 315-328, Pergamon, Tarrytown, N.Y., 1962.

Bell, J.F., III, and D. Crisp, Groundbased imaging spectroscopy of Mars in the near-infrared: Preliminary results, *Icarus, 104,* 2-19, 1993.

Bell, J.F., III, T.B. McCord, and P.D. Owensby, Observational evidence of crystalline iron oxides on Mars, *J. Geophys. Res., 95,* 14,447-14,461, 1990.

Bell, J.F., III, R.V. Morris, and J.B. Adams, Thermally altered palagonitic tephra: A spectral and process analog to the soil and dust of Mars, *J. Geophys. Res., 98,* 3373-3385, 1993.

Bell, J.F., III, M.J. Wolff, P.B. James, R.T. Clancy, S.W. Lee, and L.J. Martin, Mars surface mineralogy from Hubble Space Telescope imaging during 1994-1995: Observations, calibration, and initial results, *J. Geophys. Res., 102,* 9109-9123, 1997.

Bishop, J.L., C.M. Pieters, and R.G. Burns, Reflectance and Mössbauer spectroscopy of ferrihydrite-montmorillonite assemblages as Mars soil analog materials, *Geochim. Cosmochim. Acta, 57,* 4583-4595, 1993.

Brigatti, M.F., Relationships between composition and structure in Fe-rich smectites, *Clay Miner., 18,* 177-186, 1983.

Burns, R.G., and D.S. Fisher, Rates of oxidative weathering on the surface of Mars, *J. Geophys. Res., 98,* 3365-3372, 1993.

Butler, J.R., The geochemistry and mineralogy of rock weathering, 2, The Nordmarka area, Oslo, *Geochim. Cosmochim. Acta, 6,* 268-281, 1954.

Cabannes-Ott, C., Sur la structure de quelques hydroxydes naturels du type XOOH: Diaspore, manganite, goethite, lépidocrocite, *C. R. Acad. Sci., 244,* 2491-2494, 1957.

Caillère, S., and T. Pobeguin, Considérations sur la genèse des bauxites de la France méridionale, *C. R. Acad. Sci., 259,* 3033-3035, 1964.

Caillère, S., and T. Pobeguin, Problèmes de structures posés par la présence du fer dans les diaspores, *C. R. Acad. Sci., Ser. D, 263,* 1349-1351, 1966.

Calvin, W.M., Variation of the 3-μm absorption feature on Mars: Observations over eastern Valles Marineris by the Mariner 6 infrared spectrometer, *J. Geophys. Res., 102,* 9097-9107, 1997.

Cambier, P., Infrared study of goethites of varying crystallinity and particle size, I, Interpretation of OH and lattice vibration frequencies, *Clay Miner., 21,* 191-200, 1986.

Carr, M.H., *Water on Mars,* Oxford Univ. Press, New York, 1996.

Carroll, D., *Rock Weathering,* Plenum, New York, 1970.

Carroll, D., and J.C. Hathaway, Mineralogy of selected soils from Guam, *U.S. Geol. Surv. Prof. Pap., 403-F,* F1-F49, 1963.

Carroll, D., and M. Woof, Laterite developed on basalt at Inverell, New South Wales, *Soil Sci., 72,* 87-99, 1951.

Christensen, P.R., et al., The composition of Martian surface materials: Mars Global Surveyor Thermal Emission Spectrometer observations (abstract), *Lunar Planet. Sci.* [CD-ROM], *XXX,* abstract 1461, 1999.

Clark, B.C., Geochemical components in Martian soil, *Geochim. Cosmochim. Acta, 57,* 4575-4581, 1993.

Clifford, S.M., A model for the hydrologic and climatic behavior of water on Mars, *J. Geophys. Res., 98,* 10,973-11,016, 1993.

Coey, J.M.D., S. Morup, M.B. Madsen, and J.M. Knudsen, Titanomaghemite in magnetic soils on Earth and Mars, *J. Geophys. Res., 95,* 14,423-14,425, 1990.

Coleman, N.T., II. Decomposition of clays and the fate of aluminum, *Econ. Geol., 57,* 1207-1218, 1962.

Cornell, R.M., and U. Schwertmann, *The Iron Oxides,* 573 pp., VCH, New York, 1997.

Correns, C.W., Experiments on the decomposition of silicates and discussion of chemical weathering, in *Proceedings of the 10th National Conference on Clays and Clay Minerals,* edited by A. Swineford, pp. 443-459, MacMillan, New York, 1961.

Crowley, J.K., Near-infrared reflectance of zunyite: Implications for field mapping and remote-sensing detection of hydrothermally altered high alumina rocks, *Econ. Geol., 79,* 553-557, 1984.

Deer, W.A., R.A. Howie, and J. Zussman, *Rock-Forming Minerals, vol. 5 Non-Silicates,* 371 pp., Copp, Clark, Mississauga, Ont., 1962.

Farmer, V.C. (Ed.), *The Infrared Spectra of Minerals,* 539 pp., Mineral. Soc., London, 1974.

Frederickson, L.D., Jr., Characterization of hydrated aluminas by infrared spectroscopy: Application to study of bauxite ores, *Anal. Chem., 26,* 1883-1885, 1954.

Fripiat, J.J., H. Bosmans, and P.G. Rouxhet, Proton mobility in solids, I, Hydrogenic vibration modes and proton delocalization in boehmite, *J. Phys. Chem., 71,* 1097-1111, 1967a.

Fripiat, J.J., P.G. Rouxhet, H. Jacobs, and A. Jelli, La délocalisation des protons dans les solides inorganiques, *Bull. Groupe Fr. Argiles, 19,* 87-95, 1967b.

Fujita, T., and H. Takahashi, Formation and properties of the iron oxide zone on ion exchange, VIII, Crystal structure of hydrous ferric oxide solution prepared by using anion exchange resin, *Nippon Kagaku Zasshi, 90,* 357-360, 1969.

Geerken, R., and H. Kaufmann, Spectral effects of surface characters and rock accessories, a critical contribution to the applicability of high spectral resolution sensor data, in *Proceedings of the 9th Annual Symposium of EARSeL,* pp. 501-511, Balkema, Rotterdam, The Netherlands, 1989.

Geissler, P.E., R.B. Singer, G. Komatsu, S. Murchie, and J. Mustard, An unusual spectral unit in West Candor Chasma: Evidence for aqueous or hydrothermal alteration in the Martian canyons, *Icarus, 106,* 380-391, 1993.

Geptner, A.R., Palagonite and the process of palagonitization, *Litho. Miner. Resour., 5,* 594-607, 1970.

Glemser, O., and R. Hartert, Knickschwingungen der OH-Gruppe im Gitter von Hydroxyden, *Naturwissenschaften, 40,* 552-553, 1953.

Grove, C.I., S.J. Hook, and E.D. Paylor II, *Laboratory Reflectance Spectra of 160 Minerals, 0.4 to 2.5 Micrometers, JPL Publ. 92-2,* Jet Propul. Lab., Pasadena, Calif., 1992.

Hanlon, F.N., The bauxites of New South Wales, *R. Soc. New South Wales J. Proc., 78,* 94-112, 1944.

Harder, E.C., Stratigraphy and origin of bauxite deposits, *Bull. Geol. Soc. Am., 60,* 887-908, 1949.

Hartert, E., and O. Glemser, Ultrarotspektroskopische Bestimmung der Metall-Sauerstoff-Abstände in Hydroxyden, basischen Salzen und Salzhydraten, *Z. Elektrochem., 60,* 746-751, 1956.

Hay, R.L., and A. Iijima, Nature and origin of palagonite tuffs of the Honolulu Group on Oahu, Hawaii, *Mem. Geol. Soc. Am., 116,* 331-376, 1968.

Hunt, G.R., Near-infrared (1.3-2.4 μm) spectra of alteration minerals: Potential for use in remote sensing, *Geophysics, 44,* 1974-1986, 1979.

Hunt, G.R., and J.W. Salisbury, Visible and near-infrared spectra of minerals and rocks, 1, Silicate minerals, *Mod. Geol., 1,* 281-300, 1970.

Hunt, G.R., J.W. Salisbury, and C.J. Lenhoff, Visible and near-infrared spectra

of minerals and rocks, III, Oxides and hydroxides, *Mod. Geol., 2,* 195-205, 1971.

Jackson, M.L., Y Hseung, R.B. Corey, E.J. Evans, and R.C. Vanden Heuvel, Weathering sequence of clay-size minerals in soils and sediments, II, Chemical weathering of layer silicates, *Proc Soil Sci. Soc. Am., 16,* 3-6, 1952.

Jacob, L., Jr. (Ed.), *Bauxite, Proceedings of the 1984 Bauxite Symposium,* Am. Inst. of Min Metal Pet. Eng., New York, 1984.

Jónás, K., and K. Solymár, Determination of the mineral composition of bauxites by infrared spectrophotometry, *Acta Chim. Budapest, 66,* 1-11, 1970.

Jónás, K., K Solymár, and M. Orbán, Phase analysis and characterization of bauxites and red muds by infrared spectrophotometry, in *Proceedings of the Third International ICSOBA Congress,* pp. 325-330, Ed. Sedal, Paris, 1973

Kämpf, N , and U. Schwertmann, Goethite and hematite in a climosequence in southern Brazil and their application in classification of kaolinitic soils, *Geoderma, 29,* 27-39, 1983.

Károly, S., and J. Klára, A goethit rácsába beépült Al-tartalom vizsgálata és jelentősége a magyar bauxitokban, *Banyasz. Kohasz. Lapok Kohasz., 104,* 226-235, 1971.

Keller, W D., Observations on the origin of Missouri high-alumina clays, in *Problems of Clay and Laterite Genesis,* pp. 115-134, Am. Inst. of Min. and Eng., New York, 1952.

Keller, W D., Processes of origin and alteration of clay minerals, in *Soil Clay Mineralogy: A Symposium,* edited by C.I. Rich and G.W. Kunze, pp. 3-76, Univ. of N. Carolina Press, Chapel Hill, 1964.

Keller, W.D., and R.P. Stevens, Physical arrangement of high-alumina clay types in a Missouri clay deposit and implications for their genesis, *Clays Clay Miner., 31,* 422-434, 1983.

Keller, W.D., J.F. Westcott, and A.O. Bledsoe, The origin of Missouri fire clays, *Clays Clay Miner., 2,* 7-46, 1954.

Kennedy, G.C., Phase relations in the system Al_2O_3-H_2O at high temperatures and pressures, *Am. J. Sci , 257,* 563-573, 1959.

Kirkland, L.E., and K.C. Herr, Mariner 7 IRS revisited: Evidence for goethite on Mars, *Bull. Am. Astron. Soc., 30,* 2208, 1998.

Kiskyras, D., Die mineralogische Zusammensetzung der griechsichen Bauxite in Abhängigkeit von der Tektonik, *Neues Jahrb. Mineral. Abh., 94,* 662-680, 1960.

Kodama, H., C.R. De Kimpe, and J. Dejou, Ferrian saponite in a gabbro saprolite at Mont Mégantic, Quebec, *Clays Clay Miner., 36,* 102-110, 1988.

Kolesova, V.A., and Ya.I. Ryskin, Infrared absorption spectra of diaspore (α-AlOOH) boehmite (γ-AlOOH) and GaOOH, *Zh. Strukt. Khim., 3,* 656-659, 1962.

Kostov, I., *Mineralogy,* Oliver and Boyd, White Plains, N.Y., 1968.

Loughnan, F.C., Some considerations in the weathering of the silicate minerals, *J Sediment. Petrol., 32,* 284-290, 1962.

MacKinnon, D.J., and K.L. Tanaka, The impacted Martian crust: Structure, hydrology, and some geologic implications, *J. Geophys. Res., 94,* 17,359-17,370, 1989.

Madsen, M.B., S.F. Hviid, H.P. Gunnlaugson, J.M. Knudsen, W. Goetz, C.T. Pedersen, A.R. Dinsesen, C.T. Mogensen, M. Olsen, and R.B. Hargraves, The magnetic properties experiments on Mars Pathfinder, *J. Geophys. Res., 104,* 8761-8779, 1999.

Maksimović, Z., Genesis of some Mediterranean karstic bauxite deposits, in *Symposium on Advances in Geology, Geochemistry, and Treatment of Bauxite,* edited by R. Marušić, pp. 1-14, Izdavačky zavod Jugoslavenske akademije znanosti i umjetnosti, Zagreb, Yugoslavia, 1976.

Mao, H.K., and P.M. Bell, Crystal-field effects of ferric iron in goethite and lepidocrocite: Band assignment and geochemical applications at high pressure, *Yearbook Carnegie Inst. Washington, 73,* 502-507, 1974.

McSween, H.Y , Jr., and A.H. Treiman, Martian meteorites, in *Planetary Materials,* edited by J.J. Papike, pp. 6-1 - 6-53, Miner. Soc. of Am., Washington, D. C., 1998.

McSween, H.Y., Jr., et al., Chemical, multispectral, and textural constraints on the composition and origin of rocks at the Mars Pathfinder landing site, *J. Geophys. Res., 104,* 8679-8715, 1999.

Mead, W J , Occurrence and origin of the bauxite deposits of Arkansas, *J. Geol , 10,* 28-54, 1915.

Millot, G., and M. Bonifas, Transformations isovolumetriques dans les phénomènes de latéritisation et bauxitisation, *Bull. Serv. Carte Géol. Alsace Lorraine, 8,* 3-20, 1955.

Mindszenty, A., On the structure and texture of some diasporites, in *Symposium on Advances in Geology, Geochemistry, and Treatment of Bauxite,* edited by R. Marušić, pp. 195-197, Izdavačky zavod Jugoslavenske akademije znanosti i umjetnosti, Zagreb, Yugoslavia, 1976.

Miyamoto, M., Infrared diffuse reflectances of some hydrous minerals: Absorption bands near 3 μm (abstract), *Lunar Planet. Sci. Conf., 19,* 796-797, 1988.

Moenke, H., *Mineralspektren,* Akademie-Verlag, Berlin, 1962.

Mohr, E.C.J , and F.A. Van Baren, *Tropical Soils,* Wiley-Interscience, New York, 1954.

Morris, R.V., and D.C. Golden, Goldenrod pigments and the occurrence of hematite and possibly goethite in the Olympus-Amazonis region of Mars, *Icarus, 134,* 1-10, 1998.

Morris, R.V., H.V. Lauer Jr., C.A. Lawson, E.K. Gibson Jr., G.A. Nace, and C. Stewart, Spectral and other physicochemical properties of submicron powders of hematite (α-Fe_2O_3), maghemite (γ-Fe_2O_3), magnetite (Fe_3O_4), goethite (α-FeOOH), and lepidocrocite (γ-FeOOH), *J. Geophys. Res., 90,* 3126-3144, 1985.

Morris, R.V., D.G. Agresti, H.V. Lauer Jr., J.A. Newcomb, T.D. Shelfer, and A.V. Murali, Evidence for pigmentary hematite on Mars based on optical, magnetic, and Mössbauer studies of superparamagnetic (nanocrystalline) hematite, *J. Geophys. Res., 94,* 2760-2778, 1989.

Morris, R.V., D.C. Golden, J.F. Bell III, H.V. Lauer Jr., and J.B. Adams, Pigmenting agents in Martian soils: Inferences from spectral Mössbauer, and magnetic properties of nanophase and other iron oxides in Hawaiian palagonitic soil PN-9, *Geochim. Cosmochim. Acta, 57,* 4597-4609, 1993.

Morris, R.V., et al., Mineralogy, composition, and alteration of Mars Pathfinder rocks and soils: Evidence from multispectral, elemental, and magnetic data on terrestrial analogue, SNC meteorites, and Pathfinder samples, *J. Geophys. Res.,105,* 1757-1817, 2000.

Murchie, S., J. Mustard, J. Bishop, J. Head, and C. Pieters, Spatial variations in the spectral properties of bright regions on Mars, *Icarus, 105,* 454-468, 1993.

Mustard, J.F., and J.M. Sunshine, Seeing through the dust: Martian crustal heterogeneity and links to the SNC meteorites, *Science, 267,* 1623-1626, 1995.

Mustard, J.F., S. Erard, J-P. Bibring, J.W. Head, S. Hurtrez, Y. Langevin, C.M. Pieters, and C.J. Sotin, The surface of Syrtis Major: Composition of the volcanic substrate and mixing with altered dust and soil, *J. Geophys. Res., 98,* 3387-3400, 1993.

Nahon, D.B., Evolution of iron crusts in tropical landscapes, in *Rates of Chemical Weathering of Rocks and Minerals,* edited by S.M. Colman and D.P. Dethier, pp. 169-191, Academic, San Diego, Calif., 1986.

Nahon, D.B., and F. Colin, Chemical weathering of orthopyroxenes under lateritic conditions, *Am. J. Sci., 282,* 1232-1243, 1982.

Nahon, D., H. Paquet, and J. Delvigne, Lateritic weathering of ultramafic rocks and the concentration of nickel in the western Ivory Coast, *Econ. Geol., 77,* 1159-1175, 1982.

Nia, R., Geologische, petrographische, geochemische Untersuchungen zum Problem der Boehmit-Diaspor-Genese in griechischen Oberkriede-Bauxiten der Parnass-Kiona-Zone, Ph.D. thesis, Univ. of Hamburg, Hamburg, Germany, 1968.

Nia, R., Genesis of boehmite and diaspore Cretaceous bauxites of the Parnassos-Kiona Zone, in *ICSOBA, 2nd Symposium, vol. 2,* pp 69-98, Hungarian Academy of Sciences, Budapest, Hungary, 1969.

Nobuoka, S., X-ray and infrared absorption studies on the formation process of α-Fe_2O_3 and α-FeOOH from ferric hydroxide precipitate, *Kogyo Kagaku Zasshi, 68,* 2311-2317, 1965.

Norrish, K., and R.M. Taylor, The isomorphous replacement of iron by aluminium in soil goethites, *J. Soil Sci., 12,* 294-306, 1961.

O'Connor, J.T., Mineral stability at the Martian surface, *J. Geophys. Res., 73,* 5301-5311, 1968.

Pang, K., and J.M. Ajello, Complex refractive index of Martian dust: Wavelength dependence and composition, *Icarus, 30,* 63-74, 1977.

Patterson, S.H., H.F. Kurtz, J.C. Olson, and C.L. Neeley, World bauxite resources, *U.S. Geol. Surv. Prof. Pap., 1076-B,* 1986.

Pieters, C.M., Strength of mineral components in the transmitted component of near-infrared light: First results from RELAB, *J. Geophys. Res., 88,* 9534-9544, 1983.

Pimentel, G.C., P.B. Forney, and K.C. Herr, Evidence about hydrate and solid water in the Martian surface from the 1969 Mariner infrared spectrometer, *J. Geophys. Res., 79,* 1623-1634, 1974.

Pinet, P., and S. Chevrel, Spectral identification of geological units on the surface of Mars related to the presence of silicates from Earth-based near-infrared telescopic charge-couple device imaging, *J. Geophys. Res., 95,* 14,435-14,446, 1990.

Pollack, J.B., J.F. Kasting, S.M. Richardson, and K. Poliakoff, The case for a wet, warm climate on early Mars, *Icarus, 71,* 203-224, 1987.

Postawko, S.E., and F.P. Fanale, Changes in erosional style on early Mars: External versus internal influences, *J. Geophys. Res., 98,* 11,017-11,024, 1993.

Reflectance Experiment Laboratory (RELAB), *Reflectance Experiment Laboratory (RELAB) Description and User's Manual,* Brown Univ., Providence, R. I., 1996.

Rieder, R., H. Wänke, T. Economou, and A. Turkevich, Determination of the chemical composition of Martian soil and rocks: The alpha proton X ray spectrometer, *J. Geophys. Res., 102,* 4027-4044, 1997.

Rouquerol, J., J. Fraissard, M.-V. Mathieu, J. Elston, and B. Imelik, Étude par spectrographie infrarouge de l'eau de constitution des produits de décompositions des hydroxydes d'aluminium et de béryllium, *Bull. Soc. Chim. Fr., 12,* 4233-4237, 1970.

Roush, T.L., D.L. Blaney, and R.B. Singer, The surface composition of Mars as inferred from spectroscopic observations, in *Remote Geochemical Analysis: Elemental and Mineralogical Composition,* edited by C.M. Pieters and P.A.J. Englert pp. 367-393, Cambridge Univ. Press, New York, 1993.

Rudnitskaya, E.S., and T.A. Ziborova, Studies of bauxites by infrared spectroscopy, *Geol. Rudh. Mestorozhd., 9,* 98-103, 1967.

Ryskin, Y.I., The vibrations of protons in minerals: Hydroxyl, water and ammonium, in *The Infra-Red Spectra of Minerals,* edited by V.C. Farmer, pp. 137-181, Mineral. Soc., London, 1974.

Sabol, D.E., Jr., J.B. Adams, and M.O. Smith, Quantitative subpixel spectral detection of targets in multispectral images, *J. Geophys. Res., 97,* 2659-2672, 1992.

Sagan, C., J.P. Phaneuf, and M. Ihnat, Total reflection spectrophotometry and thermogravimetric analysis of simulated Martian surface materials, *Icarus, 4,* 43-61, 1965.

Sato, K., T. Sudo, F. Kurosawa, and O. Kammori, The influence of crystallization on the infrared spectra of α- and γ-ferric oxyhydroxides, *Nippon Kinzoku Gakkaishi, 33,* 1371-1376, 1969.

Sato, T., The thermal transformation of alumina monohydrate, boehmite, *J. Appl. Chem., 12,* 9-12, 1962.

Schwarzmann, E., Zusammenhang zwischen OH-Valenzfrequenzen und OH···OH- bzw. OH···O-Abständen in festen Hydroxiden, *Z. Anorg. Allg. Chem., 317,* 176-185, 1962.

Seelye, F.T., L.I. Grange, and L.H. Davis, The laterites of Western Samoa, *Soil Sci., 46,* 23-31, 1938.

Sherman, G.D., Factors influencing the development of lateritic and laterite soils in the Hawaiian Islands, *Pac. Sci., 3,* 307-314, 1949.

Sherman, G.D., The genesis and morphology of the alumina-rich laterite clays, in *Problems of Clay and Laterite Genesis,* Wiley-Interscience, New York, 1952.

Sherman, G.D., and H. Ikawa, Occurrence of gibbsite amygdules in Haiku bauxite area of Maui, *Pac. Sci., 13,* 291-294, 1959.

Sherman, G.D., and G. Uehara, The weathering of olivine basalt in Hawaii and its pedogenic significance, *Proc. Soil Sci. Soc. Am., 20,* 337-340, 1956.

Sherman, D.M., and T.D. Waite, Electronic spectra of Fe^{3+} oxides and oxide hydroxides in the near IR to near UV, *Am. Mineral., 70,* 1262-1269, 1985.

Sherman, D.M., R.G. Burns, and V.M. Burns, Spectral characteristics of the iron oxides with application to the Martian bright region mineralogy, *J. Geophys. Res., 87,* 10,169-10,180, 1982.

Siever, R., and N. Woodford, Dissolution kinetics and the weathering of mafic minerals, *Geochim. Cosmochim. Acta, 43,* 717-724, 1979.

Sijarić, G., F. Trubelja, and S. Šćavničar, Diaspore bauxites of the Gremč Mountain, Bosnia, in *Proceedings of the 13th International ICSOBA Congress,* pp. 115-124, l'Académie Yougoslave des Sciences et des Arts, Zagreb, Yugoslavia, 1973.

Silverstein, R.M., G.C. Bassler, and T.C. Morrill, *Spectrometric Identification of Organic Compounds,* 5th ed., 419 pp., John Wiley, New York, 1991.

Singer, R.B., Spectral evidence for the mineralogy of high-albedo soils and dust on Mars, *J. Geophys. Res., 87,* 10,159-10,168, 1982.

Singer, R.B., Spectroscopic observations of Mars, *Adv. Space Res., 5,* 59-68, 1985.

Singer, R.B., T.B. McCord, R.N. Clark, J.B. Adams, and R.L. Huguenin, Mars surface composition from reflectance spectroscopy: A summary, *J. Geophys. Res., 84,* 8415-8426, 1979.

Soderblom, L.A., The composition and mineralogy of the Martian surface from spectroscopic observations: 0.3 to 50 μm, in *Mars,* edited by H.H. Kieffer et al., Univ. of Ariz. Press, Tucson, 1992.

Solymár, K., and K. Jónás, A goethit rácsába beépült Al-tartalom vizsgálata és jelentősége a magyar bauxitokban, *Banyasz. Kohasz. Lapok Kohasz., 104,* 226-235, 1971.

Squyres, S.W., and J.F. Kasting, Early Mars: How warm and how wet?, *Science, 265,* 744-748, 1994.

Stumpf, H.C., A.S. Russell, J.W. Newsome, and C.M. Tucker, Thermal transformation of aluminas and alumina hydrates, *Ind. Eng. Chem., 42,* 1398-1403, 1950.

Tiller, K.G., The geochemistry of basaltic materials and associated soils of south-eastern South Australia, *J. Soil Sci., 9,* 225-241, 1958.

Townsend, T.E., Discrimination of iron alteration minerals in visible and near-infrared reflectance data, *J. Geophys. Res., 92,* 1441-1454, 1987.

Tsuchida, T., and K. Kodaira, Hydrothermal synthesis and characterization of diaspore, β-$Al_2O_3 \cdot H_2O$, *J. Mater. Sci., 25,* 4423-4426, 1990.

Ugolini, F.C., Processes and rates of weathering in cold and polar desert environments, in *Rates of Chemical Weathering of Rocks and Minerals,* edited by S.M. Colman and D.P. Dethier, pp. 193-235, Academic, San Diego, Calif., 1986.

Valeton, I., *Bauxites,* Elsevier Sci., New York, 1972.

Vempati, R.K., R.V. Morris, and H.V. Lauer Jr., Spectral properties of Cr substituted goethites and hematites (abstract), *Lunar Planet. Sci. Conf., 23,* 1465-1466, 1992.

Vempati, R.K., R.V. Morris, H.V. Lauer Jr., and P.A. Helmke, Reflectivity and other physicochemical properties of Mn-substituted goethites and hematites, *J. Geophys. Res., 100,* 3285-3295, 1995.

Vlasov, A.Y., G.V. Loseva, G.S. Sakash, and L.S. Solntsev, The study of temperature transformation of α-ferric oxyhydroxide to hematite by the method of infrared spectroscopy, *Zh. Prikl. Spektrosk., 12,* 1130-1133, 1970.

Wayman, C.H., Solid-gas interface in weathering reactions, in *Proceedings of the 11th National Conference on Clays and Clay Minerals,* edited by A. Swineford, pp. 84-94, MacMillan, New York, 1963.

Wefers, K., Zur chemischen Technologie des Bauxitaufschlusses Teil I: Das System Na_2O-Al_2O_3-H_2O, *Metallography, 21,* 1-10, 1967a.

Wefers, K., Phasenbeziehungen im System Al_2O_3-Fe_2O_3-H_2O, *Erzmetall, 20,* 13-19, 1967b.

Wefers, K., Phasenbeziehungen im System Al_2O_3-Fe_2O_3-H_2O, *Erzmetall, 20,* 71-75, 1967c.

Wolska, E., and U. Schwertmann, The mechanism of solid solution formation between goethite and diaspore, *Neues Jahrb. Mineral. Monatsch., H.5,* 213-223, 1993.

J. F. Bell III, Department of Astronomy, Cornell University, Ithaca, NY 14853.

E. A. Cloutis (corresponding author), Department of Geography, University of Winnipeg, 515 Portage Avenue, Winnipeg, Manitoba, Canada R3B 2E9. (e.cloutis@uwinnipeg.ca)

(Received September 24, 1999; revised December 22, 1999; accepted January 4, 2000.)